NASA-CR-163096
19810012480

NASA Contractor Report 163096

FLOW VISUALIZATION STUDY OF SPANWISE BLOWING APPLIED TO THE F-4 FIGHTER AIRCRAFT CONFIGURATION

Dale J. Lorincz

Contract NAS4-2616
August 1980

NASA

NASA Contractor Report 163096

FLOW VISUALIZATION STUDY OF SPANWISE BLOWING APPLIED TO THE F-4 FIGHTER AIRCRAFT CONFIGURATION

Dale J. Lorincz
Northrop Corporation
Hawthorne, California

Prepared for
Dryden Flight Research Center
under Contract NAS4-2616

National Aeronautics and
Space Administration

Scientific and Technical
Information Office
1980

Intentionally Left Blank

CONTENTS

CONTENTS (Continued)

SUMMARY

Water tunnel studies have been performed to qualitatively evaluate the benefits of spanwise blowing applied to the F-4 fighter aircraft. Particular emphasis was placed on defining the changes that occur in the vortex flow fields above the wing due to spanwise blowing over the inboard and outboard wing panels and over the trailing-edge flaps. The flow visualization tests were conducted in the Northrop water tunnel using a 1/48-scale model of the F-4. Flow visualization photographs were obtained over an angle of attack range of from 10° to 30° at sideslip angles of 0° and 10°.

Spanwise blowing on the F-4 model was investigated in detail to determine the sensitivity of the vortex flows to changes in flap deflection angle, nozzle position, and jet momentum coefficient. Leading-edge and trailing-edge flap settings for two landing configurations and one maneuver configuration were tested. The leading-edge flap deflection of 30° for the landing configuration delayed flow separation and the formation of the wing vortex to higher angles of attack. When spanwise blowing was applied aft of the flap hinge line, the flow separated at the knee of the flap and a stable vortex was formed. Increasing the blowing rate was found to delay the breakdown of the wing vortex to farther outboard and to higher angles of attack. When the innermost

segment of the leading-edge flap was left undeflected, a leading-edge vortex was formed at a lower angle of attack. The lift enhancement due to spanwise blowing stabilizing the vortex then begins at a lower angle of attack. Spanwise blowing over the trailing-edge flap, deflected 60° for landing, entrained flow downward, which produces a lift increase over a wide range of angles of attack.

The sweep angle of the windward wing was effectively reduced in sideslip. This decreased the stability of the vortex, and it burst farther inboard. Reduced wing sweep required a higher blowing rate to maintain a stable vortex. A vortex was stabilized on the outboard wing panel for a maneuver configuration using an outboard nozzle. Blowing from both an inboard and an outboard nozzle was found to have a favorable interaction.

INTRODUCTION

Chordwise blowing from the knees of both the leading-edge and trailing-edge flaps is currently employed on the F-4. This acts to control the boundary layer, delaying boundary-layer separation to higher angles of attack and increasing lift during approach and landing. Both effects serve to reduce approach speeds. Lift can also be increased by a jet blowing

spanwise from the fuselage. As the flow separates at the leading edge of a thin, swept wing, it rolls up into a spiral vortex. On a wing of moderate sweep, such as that of the F-4, the leading-edge vortex breaks down above the wing at moderate angles of attack. By blowing spanwise near the leading edge and approximately parallel to it, the vortex being shed at the leading edge is trapped over the wing in the area ahead of the jet. The increased spanwise flow along the axis of the vortex aids in the formation of a stable vortex on wings of moderate sweep and delays the vortex breakdown to farther outboard on the wing and to higher angles of attack. By delaying the breakdown, the low pressure associated with the leading-edge vortex is maintained, causing an increase in the vortex lift (References 1 to 6).

The use of a blowing nozzle outboard on the wing could result in a reduction in the amount of blowing required to stabilize the flow. The blowing is applied where the wing first stalls and the area that the jet must cover is much smaller. Spanwise blowing over a wing panel outboard of a snag similar to the F-4 has been shown in Reference 7 to reduce the pressure fluctuations associated with transonic buffet. Spanwise blowing has also been shown to reduce the severity of the low speed, high angle of attack wing rock on a fighter aircraft in free flight model tests (Reference 8).

Spanwise blowing can also be applied over trailing-edge flaps. This will act as a boundary layer control device through flow entrainment. Away from the boundary layer there is also a strong downwash over the flap as the jet entrains the far field flow downward. Spanwise blowing across trailing-edge flaps has been shown to be equally effective at increasing the lift for landing as chordwise blowing from the knee of the flap (Reference 9). A spanwise blowing system using the same engine compressor bleed air as the chordwise blowing system would weigh less, be simpler, and be more reliable because it does not require the complicated air ducting and blowing slots in the wing.

This flow visualization study was undertaken to provide a qualitative evaluation of the benefits of spanwise blowing. All testing for this study was done in the Northrop water tunnel which has a test section of 0.41 by 0.61 meters. Changes in angle of attack, sideslip, and model configuration can be made quickly and inexpensively using small scale models. The flow visualization results discussed in this report were obtained using a 1/48-scale model of the F-4C/D. Studies done at Northrop using the water tunnel have provided excellent visualization of vortex flows on wings and fuselage forebodies. The water tunnel has been used to qualitatively define the vortex flow fields on many aircraft configurations.

The primary purpose of these tests was to define the changes that occur in the vortex flow fields generated above the wing due to spanwise blowing in order to qualitatively assess the benefits of spanwise blowing. The sensitivity of the vortex flows to changes in angle of attack and sideslip, flap deflection angle, nozzle chordwise location, and jet momentum coefficient was determined. Wherever possible, the water tunnel results are compared to unpublished wind tunnel data from the McDonnell Aircraft Co. low-speed wind tunnel on an F-4C/D model.

SYMBOLS

C_L	lift coefficient
C_{L_T}	trimmed lift coefficient
C_μ	jet momentum coefficient, $\dot{w}\ V_j/g\ q_\infty\ S$
c_h	inboard wing panel chord at wing hinge
c_r	exposed wing root chord
d	nozzle diameter
g	gravitational acceleration
h	height of nozzle center line above upper surface
$\dot{m}_I$	mass flow to inlet
$\dot{m}_\infty$	capture mass flow

q_∞	freestream dynamic pressure
S	wing reference area
V_j	jet velocity
$\dot{w}$	nozzle weight flow rate
x	chordwise distance from leading edge
α	angle of attack of wing
β	angle of sideslip
δ_n	leading-edge flap deflection
δ_f	trailing-edge flap deflection
Λ_{LE}	leading-edge sweep angle
Λ_N	nozzle sweep angle

EXPERIMENTAL METHODS

Water Tunnel Facility

The Northrop water tunnel is a closed return tunnel used for high quality flow visualization of complex three-dimensional flow fields. The water tunnel is shown schematically in Figure 1. The test section is 0.41 m by 0.61 m by 1.83 m long and has walls made of transparent Plexiglas. The test section is oriented in the vertical direction, which permits the model to be viewed from any angle. A model is shown installed in the test section in Figure 2. The model is accessed through the

top of the tunnel by means of suspension cables connected to the model support system.

The model support system consists of a sting and sideslip arc which is capable of pitch angles from -10° to 70°, concurrent with sideslip range of -20° to 20°. The sideslip angle is fixed prior to the model installation. The pitch angle is then manually adjusted from the side of the test section.

Test Procedure

The flow visualization in the water tunnel is obtained by injecting colored food dyes having the same density as water. The density of water is 800 times that of air, which gives the dye excellent light reflecting characteristics relative to using smoke in air. The dye is introduced into the flow field through small orifices and dye tubes distributed along the body of the model. The dye can also be introduced through a dye probe, which can be accurately positioned at any point in the test section by means of a traversing mechanism.

Inlet flows are simulated in the water tunnel by applying suction to tubes connected to the rear of the model's exhaust nozzles. The tubes are run to a water flow meter outside the tunnel. Flow meters are used to accurately measure

and set the inlet flow rate and any jet blowing rates. The water tunnel is operated at a test section velocity of 0.1 meters/second which has been found to produce the best flow visualization results. This velocity corresponds to a Reynolds number of 1×10^5/meter.

VORTEX FLOW FIELDS

Prior to the development of the Northrop water tunnel, the question of whether vortex flow fields in air could be properly simulated in water with sufficient accuracy was considered. It is well known that if cavitation is avoided and compressibility effects are negligible, the fluid motions of water and air at the same Reynolds number are dynamically similar. For identical model scale and velocity, the Reynolds number in water is higher by a factor of 15. However, because of practical limitations in speed and model scale, water tunnel tests are generally run at Reynolds numbers well below those in wind tunnels.

For thin, swept wings, boundary layer separation occurs along the sharp leading edge. The sheet of distributed vorticity that is shed rolls up into a spiral vortex with a concentrated core. A laminar separation will occur at the sharp leading edge of the wing at the Reynolds numbers that are encountered in flight and in the water tunnel. The vortex

generation is therefore not sensitive to Reynolds number and the vortex formed in the water tunnel is representative of flight (References 10, 11, and 12).

Once the leading-edge vortex flow has formed, its stability can be affected by external conditions. At high angles of attack, the vortex core can undergo a sudden expansion, which is referred to as vortex breakdown or burst. Above the stalled portion of a wing and at the wing trailing edge, there is a large adverse pressure gradient. This negative velocity gradient will reduce the axial velocity within the core of the vortex. The vortex will then burst with a rapid expansion to a larger, slower rotating flow. The breakdown of the vortex core depends on the magnitude of the rotational and axial velocities, the external pressure gradient, and the degree of flow divergence. Studies of vortex stability have shown that the external pressure gradient is a dominant parameter for vortex burst. Therefore, when a leading-edge vortex encounters a large adverse pressure gradient above a wing it will break down in a similar manner in the water tunnel as in the wind tunnel and in flight.

The rolled-up vortex sheet induces large suction pressures on the upper surface of the wing which produce additional lift. An increase in the rotational velocity of the vortex will induce lower pressures on the surface and increase the vortex lift. At the same time, an increase in rotational velocity decreases the stability of the vortex, making it more likely to burst. A moderate increase in the axial velocity of

a vortex will increase the stability of the vortex and delay any breakdown.

The influence of Reynolds number on the vortex breakdown position has been investigated at Northrop and by others. In the Northrop studies (Reference 10), the angle of attack at which vortex breakdown occurred at the trailing edge was observed on delta wings having leading-edge sweep angles of 55° to 85°. Figure 3, which is taken from Reference 10, shows that the results obtained in the Northrop water tunnels fall within the range of angles of attack observed by others. The data shown include results from other water tunnels as well as wind tunnels and covers the Reynolds number range of 10^4 to 10^6, based on root chord. Note that the variation in the data due to Reynolds number is no greater than the variation associated with different facilities and different flow visualization techniques at the same Reynolds number. All of the data follow the same trend of increasing angle of attack for vortex breakdown at the trailing edge as the leading-edge sweep angle is increased.

The vortex burst locations above the upper surface of thin, swept wings in the water tunnel are in good agreement with the results at higher Reynolds number in wind tunnels at moderate to high angles of attack because the external pressure gradient is the dominant effect. Surface flows at low angles of attack that are not yet vortex dominated can be more sensitive to Reynolds number effects. Early laminar separation in

the water tunnel on leading-edge flaps can result in a smaller delay of vortex breakdown compared to wind tunnel results.

MODEL DESCRIPTION

The water tunnel flow visualization studies were conducted with a 1/48-scale model of the F-4C/D. A three-view drawing of the model is shown in Figure 4. The model configuration tested was with the landing gear up and all control surfaces at zero deflection. The wing was fitted with a leading-edge flap which could be deflected from 0° to 30°. The three spanwise segments of the leading-edge flap could be deflected as a unit or individually. The wing was also fitted with a trailing-edge flap that could be deflected from 0° to 60°.

The model was built with flow-through ducts from the inlets to the exhaust nozzles. To provide the desired inlet mass flow rate, a suction tube was connected to each exhaust nozzle. A sting was installed between the suction tubes on the lower surface of the model. The inlet mass flow ratio was set to simulate the inlet conditions for the military power setting at a freestream Mach number of 0.3. This mass flow ratio at zero angle of attack is $\dot{m}_I/\dot{m}_\infty = 1.2$. The mass flow would be pulled in from an area larger than the capture area of the inlet.

In order to visualize the flow field, the model was equipped with dye injection orifices. Great care was taken in locating the dye orifices to insure that dye introduced into the external flow would be entrained into the vortices. A traversing dye probe was used to survey the model to find the exact location for each orifice. For the vortex flow of the inboard wing panel, dye orifices were located near the wing apex on both the underside of the wing and on the upper surface. For the outboard wing panel, a dye orifice was installed flush with the surface at a point just aft and outboard of the snag. A dye orifice was also located flush to the upper surface of the wing and just forward of the trailing-edge flap. Dye can also be added to the water supply of the spanwise-blowing jets to show the expansion of the jet and the extent of its outboard penetration.

The fuselage and the outboard wing panel were slotted to permit a variation of the chordwise locations of the nozzles. The nozzle positions illustrated in Figure 5 are the blowing configurations evaluated in this study. The nozzles were located symmetrically right side to left and blowing was applied to both sides throughout the tests. The details of nozzle geometry and position are given in Table 1.

RESULTS AND DISCUSSION

The experimental results that were obtained from the water tunnel flow visualization studies consist of a set of photographs documenting the flow field of the F-4 for the various blowing configurations that were tested. Selected results are referred to in the text and are given at the end of this report. The changes in the wing flow field with spanwise blowing are discussed for angles of attack from 10° to 30° and for a range of jet momentum coefficients. Whenever possible, comparisons are made between the water tunnel flow visualization results and the force data obtained in the McDonnell Aircraft Co. low-speed wind tunnel.

Spanwise Blowing Over Inboard Wing in Landing Configuration

The basic landing configuration for this study has a leading-edge flap deflection of 30° and the trailing-edge flap deflected to 60°. The flow field of the wing in this landing configuration at zero sideslip is presented in Figure 6. The dye orifices near the apex of the wing and the snag are located such that the dye from them could be entrained into any vortices. At 10° angle of attack and zero jet momentum coefficient, $C_\mu = 0$, the dye being ejected is within the boundary layer and is attached on the upper surface. Figure 6 shows that there is spanwise spreading of the surface flow across the

inboard wing panel. Downstream of the snag, the flow is very unsteady. In Reference 9 it was found that flow separation starts inboard of the snag and then progresses inboard with increasing angle of attack.

The dye ejected on the leading-edge flap has less spanwise travel at 15° angle of attack and no blowing. The dye ejected ahead of the trailing-edge flap is close to the wing upper surface and is pulled spanwise toward the separated flow. Aft of the leading-edge flap, the flow is unsteady over the outboard wing panel. With increasing angle of attack, the separated flow region extends farther inboard. At 20° angle of attack, spanwise flow is seen on the surface of the leading-edge flap with the flow separating inboard at the flap knee and farther outboard near the leading edge. The separation near the leading edge occurs farther inboard on the flap at 25° angle of attack. A large, slowly rotating wake is now present above most of the wing.

A blowing nozzle was positioned first at $x/c_r = 0.3$, which is behind the flap hinge line. The effects of spanwise blowing from this nozzle are presented in Figure 6 for angles of attack from 10° to 25° and blowing rates of $C_\mu = 0.01$, 0.03, and 0.06. The blowing rate of 0.06 is near the maximum available for low flight speeds at maximum thrust. The flow over the inboard wing panel is attached at 10° angle of attack. The flow is straight aft until it is entrained into the jet. With increasing blowing rate, the jet expands farther forward and

the dye is entrained sooner into the jet at both 10° and 15° angles of attack in Figure 6. Increasing the blowing rate also enables the jet to penetrate farther outboard before it is turned streamwise by the cross-flow. At the highest blowing rate at 10° angle of attack, a weak vortex forms ahead of the jet and aft of the flap hinge line on the outboard wing panel. The outboard wing panel is stalled by 15° angle of attack and the vortex is no longer formed.

Downstream of the jet the flow was found to reattach to the surface. If the jet is thought of as a solid body, it would produce an effective increase in wing camber. This jet camber effect, discussed in References 2 and 4, can produce a lift increase at low angles of attack. Downstream of the jet and ahead of the trailing-edge flap, the flow becomes much more streamwise with spanwise blowing at both 10° and 15° angles of attack. By providing smooth, chordwise flow over the trailing edge, spanwise blowing may improve the effectiveness of the trailing-edge flap.

With no blowing and at 20° angle of attack, no vortex flow is above the wing. At the lowest blowing rate tested of 0.01, a vortex is formed aft of the flap knee and ahead of the jet. In the central region of the wing the flow separates at the flap knee and then rolls up into the vortex. Increasing the blowing to C_μ = 0.03 at 20° angle of attack pushes the vortex closer to the leading edge. The higher blowing rate delays the vortex bursting to farther outboard and increases

its apparent strength, as was evident in the increased rotational velocity. At 20° angle of attack, the jet is able to expand farther forward and extend farther outboard than at 15°. With increasing angle of attack, the jet is shielded by the wing from the freestream flow. At the highest blowing rate of 0.06, the vortex is located closer to the leading edge although it is still aft of the flap hinge line. The increased blowing rate delayed the vortex burst farther spanwise, caused the vortex to roll up tighter, decreasing its size, and decreased the vertical displacement of the vortex above the upper wing surface.

A vortex forms on the wing at 25° angle of attack for only the highest blowing rate of 0.06. The vortex burst point is displaced inboard relative to that seen at 20° angle of attack for the same blowing rate. At the blowing rate of 0.03 at 25° angle of attack, the flow near the leading edge is more spanwise and shows less reversed flow than with blowing off but no vortex is formed. The flow ahead of the trailing-edge flap continues in a chordwise direction with the blowing on. It is evident from Figure 6 that when the angle of attack is increased, a higher blowing rate is required for a stable vortex to form at a given spanwise station.

The effect of spanwise blowing with the nozzle located at $x/c_r = 0.13$ is shown in Figure 7 for 20° and 25° angles of attack and several blowing rates. In this and all subsequent figures, dye is injected into the flow on the underside of the

wing such that it will move to the upper surface near the apex of the wing at high angles of attack. At low angles of attack, the effects on the flow field of blowing at x/c_r = 0.13 are similar to those seen for x/c_r = 0.13 except that a vortex is not generated on the outboard wing panel at 10° angle of attack. At 20° and 25° angle of attack, the flow ahead of the trailing-edge flap is more spanwise than with the nozzle at x/c_r = 0.3 in Figure 6.

A vortex forms on the wing at 20° angle of attack and x/c_r = 0.13 for only the highest blowing rate of 0.06. This vortex ahead of the jet is very weak and diffuse. No vortex flow is evident in Figure 7 at 25° angle of attack. The nozzle location of x/c_r = 0.13 places the nozzle almost directly above the flap hinge line. The flow does not separate at the flap knee but is entrained into the jet instead. Without the separation at the knee to initiate the vortex, the vortex formation is delayed to higher angles of attack where separation occurs at the leading edge. With the leading-edge flaps deflected on the fighter configuration of Reference 3, the largest lift increase was obtained with the blowing nozzle aft of the flap hinge line. When separation occurs at the flap knee, the vortex system forms farther aft of the leading edge than it would when the leading-edge flap is undeflected.

The effect of spanwise blowing on the trimmed lift coefficients of the F-4 is presented in Figure 8. The inboard segment of the wind tunnel model's leading-edge flap was

deflected to 30° which is the same as the entire flap on the water tunnel model. The trailing-edge flap was deflected to 45° instead of the 60° used in the water tunnel. The trends shown in these data should illustrate the effects of blowing as seen on the water tunnel model with δ_n/δ_f = 30°/60°.

A lift increase due to a spanwise blowing rate of 0.03 is seen in Figure 8 to occur at low angles of attack where no vortex flow was seen in the water tunnel. This lift increase is attributed to an effective increase in camber due to the presence of the jet and to an increase in trailing-edge flap effectiveness. The lift increase due to wing spanwise blowing with a deflected trailing-edge flap was found in Reference 5 to be greater than the sum of the lift of the spanwise blowing and of the deflected flap acting alone. The nonlinear increase in lift with increasing angle of attack that is characteristic of vortex enhancement does not begin until 18° angle of attack. It was at this angle of attack that a vortex was first formed aft of the flap hinge line and ahead of the jet. The vortex can be seen at 20° angle of attack for C_μ = 0.03 in Figure 6.

The effect of spanwise blowing on the lift of the clean configuration is shown in Figure 9. These data are shown only for comparison with the other wind tunnel data from the McDonnell Aircraft Co. low-speed wind tunnnel, since the clean configuration, no flap deflections, was not tested in the water tunnel. Without the trailing-edge flap deflected, the lift increase due to blowing at low angles of attack is much less

and is due only to the jet camber effect. Increasing C_μ from 0.01 to 0.03 increased the maximum lift and the angle of attack for maximum lift. Without the leading-edge flap deflected, the maximum lift increase due to blowing in Figure 9 occurs at 24° angle of attack for C_μ = 0.03. With the leading-edge flap deflected, the maximum lift increase due to spanwise blowing does not occur until 34° angle of attack in Figure 8. Since the deflection of the leading-edge flap delays separation, the beneficial effects of spanwise blowing are delayed to higher angles of attack at which the flow first separates at the flap knee and then at the leading edge.

Spanwise Blowing Over Wing and Trailing-Edge Flap in Landing Configuration

The effects of spanwise blowing over the trailing-edge flap with the nozzle located at x/c_r = 0.88 and the flaps in the landing configuration of δ_n/δ_f = 30°/60° are shown in Figure 10. The flow ahead of the flap is entrained into the jet for all of the blowing rates tested at both 10° and 15° angle of attack. The flow ahead of the flap is pulled downward around the knee of the flap to the jet where it is entrained. The flow then continues out spanwise above the flap until it reaches the tip of the flap. Once past the end of the flap, the jet is turned downstream by the freestream flow.

The dye ejected near the apex of the wing is at a greater height above the surface when it reaches the trailing-edge flap than the dye ejected just ahead of the flap. For the lowest blowing rate of 0.01 at 15° angle of attack the flow farther above the surface is pulled downward without being entrained directly into the jet. This downward motion of a large mass of fluid produces a lift increase (Reference 9). With increasing blowing rate, the dye from near the wing apex is pushed outboard of the outer edge of the trailing-edge flap. When dye was added to the blowing jet, it was seen that as the jet expanded outward, part of the jet flow passed over the top of the wing rather than under it. This could be avoided if the nozzle sweep back angle was increased or if the chordwise position along the flap was farther aft. The nozzle was tested with its axis parallel to the flap hinge line at a chordwise position of 18% of the flap chord and 88% of the wing root chord.

At 20° angle of attack, the spanwise flow directly ahead of the trailing edge flap was decreased with increasing blowing rate. At the highest blowing rate of 0.06, a weak and unsteady vortex was shed from the knee of the flap. No vortex is seen above the wing in Figure 10 for the blowing off case at 20° angle of attack. Despite much of the wing being stalled at 25° angle of attack, the spanwise blowing over the trailing-edge flap still entrains flow downward from ahead of the flap.

During an approach and landing, both the spanwise blowing over the inboard wing panel and over the trailing-edge flap would be used to increase the lift and thereby reduce the approach speed. The effects of spanwise blowing from nozzles located at x/c_r = 0.3 and 0.88 with the flaps in the landing configuration of δ_n/δ_f = 30°/60° are shown in Figure 11. The flow from near the apex of the wing is entrained into the jet at 10° and 15° angle of attack just as it was with the forward jet along in Figure 6. At the highest blowing rate of C_μ = 0.06/0.06 for the forward and aft nozzles, a weak vortex was again formed ahead of the forward jet on the outboard wing panel at 10° angle of attack. The flow ahead of the trailing-edge flap was turned chordwise with just the blowing from the forward nozzle as seen in Figure 6. However, when the flow reached the flap it separated from the surface and was turned toward the freestream direction. With the spanwise blowing over the trailing-edge flap, the flow turns around the knee of the flap, is pulled downward, and entrained into the jet.

Blowing from the aft nozzle appears in Figure 11 to have little effect on the vortex which forms ahead of the forward jet at 20° angle of attack. In both Figure 6 with the forward nozzle alone and in Figure 11, the vortex is seen to move closer to the leading edge, to burst farther outboard, and to be further enhanced with increasing blowing rate at 20° angle of attack. The blowing over the trailing-edge flap does, however, have a beneficial effect on the wing vortex at

25° angle of attack. With a blowing rate of C_μ = 0.03/0.03, a vortex was formed ahead of the forward jet where none was formed at 25° angle of attack for the forward jet alone. At the highest blowing rate, the vortex bursting is delayed to farther outboard when spanwise blowing over the trailing-edge flap is applied. The spanwise blowing would reduce the adverse pressure gradient over the flap and improve the flow field in the vicinity of the flap. An example of the premature vortex breakdown due to a deflected trailing-edge flap is given in Reference 10. In Figure 11 at 25° angle of attack for C_μ = 0.06/0.06, a dividing streamline can be seen between the vortex and the jet. Part of the dye is swept underneath the vortex and moves forward to between the vortex and the leading edge. The remainder of the dye moves aft and is entrained into the jet.

The effect of spanwise blowing over the wing and trailing-edge flap on the trimmed lift coefficients of the F-4 is presented in Figure 12. The inboard segment of the leading-edge flap was deflected to 20° in the wind tunnel which is 10° less than the 30° flap setting in the water tunnel. The trailing-edge flap setting of δ_f = 60° is the same for both models. A large lift increase at low angles of attack is produced with spanwise blowing of C_μ = 0.01/0.02. The largest percentage of this lift increase is due to the blowing over the trailing-edge flap. For angles of attack above about 18°, the forward spanwise blowing over the wing will begin to enhance

the wing vortex and thereby produce a vortex-induced lift increment.

Spanwise Blowing Over Wing and Trailing-Edge Flap in Alternate Landing Configuration

It can be seen in Figures 6 and 11 that the forward spanwise blowing jet is most effective at stabilizing the wing vortex over the inboard portions of the wing. It was suggested in Reference 5 that with segmented leading-edge flaps, the inboard flap segment could be left undeflected since the jet is most effective at stabilizing the vortex there. Farther outboard the flap segments would be deflected to maintain attached flow near the leading edge. Such a configuration was tested in the water tunnel with the inboard flap segment undeflected and the two outboard flap segments deflected 30° (δ_n = 0°/30°/30°). The 60° deflection of the trailing-edge flap was retained as was the spanwise blowing over the flap from x/c_r = 0.88. The forward blowing nozzle was moved forward to x/c_r = 0.13 because the flow will not separate at low angles of attack at the leading edge rather than farther aft at the flap hinge line. The effects of spanwise blowing on the flow field of this alternate landing configuration are illustrated in Figure 13.

At 12° angle of attack and no blowing, the flow that separates at the leading edge of the inboard flap segment rolls

up into a vortex. Figure 6 shows that with the inboard flap segment deflected to 30°, no vortex was formed at angles of attack of 10° to 15° even with spanwise blowing. Spanwise blowing of C_μ = 0.024/0.018 at 12° angle of attack is seen in Figure 13 to shift the existing vortex farther forward and outboard. The blowing rates of C_μ = 0.024/0.018 are representative of what is available from engine compressor bleed for the F-4 under approach conditions. At the higher blowing rate of C_μ = 0.06, the dye is entrained directly into the jet rather than into the leading-edge vortex.

Increasing the angle of attack from 12° to 15° with no blowing causes the burst point of the leading-edge vortex to move forward. With spanwise blowing at 15° angle of attack, the leading-edge vortex is shifted closer to the leading edge and the vortex breakdown is delayed to farther outboard. With the vortex burst point moved farther outboard, a larger wing area will be affected by the flow reattachment which occurs inboard and downstream of the vortex. There appears to be a limit to the spanwise displacement due to blowing of the leading-edge vortex. At the highest blowing rate of C_μ = 0.06/0.06, the vortex is turned sharply toward the streamwise direction at the end of the undeflected leading-edge flap segment.

Figure 13 shows that at 20° angle of attack and without blowing, the leading-edge vortex bursts near the apex of the wing. With spanwise blowing, the vortex bursting is

delayed to farther across the span of the undeflected flap segment. An increase in vortex strength is evident in the vortex becoming more concentrated with increased rotational velocity. The burst point of the leading-edge vortex with blowing off reaches the apex of the wing at 22° angle of attack, and the stalled wing is seen in Figure 13 at 25° angle of attack. When the spanwise blowing is applied, a vortex is formed ahead of the jet at 25° angle of attack. The burst point of the vortex is only slightly inboard of where it occurred at 20° angle of attack for the same blowing rates.

The effect of spanwise blowing over the wing and trailing-edge flap on the lift coefficients of the F-4 is presented in Figure 14 for a range of inboard leading-edge flap segment deflection angles. Without spanwise blowing, increasing the deflection of a leading edge flap would tend to increase the maximum lift coefficient. At high angles of attack, a deflected leading edge flap would maintain attached flow near the leading edge and thereby delay the stall of the wing. With spanwise blowing, the effect of flap deflection on lift is seen in Figure 14 to be just the opposite. The lift coefficients are reduced when the inboard flap segment is deflected. For the configuration of δ_n = 0°/60°/60°, which is similar to the alternative landing configuration of Figure 13, a leading-edge vortex is able to form at relatively low angles of attack. The favorable lift enhancement due to stabilizing the leading-edge vortex by spanwise blowing can then begin at a lower angle of

attack. Deflection of the leading edge flap was seen in the water tunnel to delay the formation of the vortex to higher angles of attack. This will delay the increase in vortex induced lift due to spanwise blowing to a higher angle of attack. The angle of attack for maximum lift would also tend to be higher for larger leading-edge flap deflections with spanwise blowing. This is the case in Figure 14 where the angle of attack for maximum lift is delayed by 10° from 21° angle of attack for δ_n = 0°/60°/60° to 31° angle of attack for δ_n = 30°/60°/60°. When the vortex is formed above the flap itself, rather than aft of the flap hinge line, a reduction in lift coefficient can occur due to the deflection of the leading edge. The vortex lift vector would rotate forward as the flap is deflected downward. This would reduce the lift but also reduce the drag.

Spanwise Blowing on Landing Configuration in Sideslip

The results obtained for the model at 10° of sideslip with flap deflections of δ_n/δ_f = 30°/60° are presented in Figure 15 for spanwise blowing from nozzles located at x/c_r = 0.3 and 0.88. With no blowing at 10° angle of attack, the dye on the upper surface of both the leeward and windward inboard wing panels shows some spanwise motion that is directed outboard. The lowest blowing rate of C_μ = 0.01/0.01 causes the flow over the inboard wing panels and ahead of the trailing-

edge flaps to turn to a more chordwise direction. With the highest blowing rate of C_μ = 0.06/0.06 at 10° angle of attack, the flow ahead of both trailing-edge flaps becomes even more chordwise. At these same conditions, a vortex forms ahead of the forward jet and aft of the leading-edge flap hinge line on the leeward, outboard wing panel. This vortex is well defined and it bursts ahead of the trailing edge. A comparison with Figure 11 for the same flap deflections and the highest blowing rate shows that at zero sideslip and 10° angle of attack, an unsteady vortex was formed, that burst after a short distance. The leeward wing in sideslip is at an effectively higher sweep angle. The increased sweep angle increases the stability of the vortex being formed enabling it to travel farther downstream before it bursts. The leading-edge sweep angle is effectively reduced on the windward side. This decreases the stability of the vortex on the windward side, causing it to burst farther forward.

On the outboard wing panel the flow aft of the leading-edge flap is unsteady at 15° angle of attack with no blowing. For a blowing rate of C_μ = 0.01/0.01 there is little change in the outboard flow. Over the inboard wing panel the blowing directs the flow more in the chordwise direction. A vortex is formed over the outboard wing panel on the leeward side for the highest blowing rate of C_μ = 0.06/0.06. The vortex breaks down farther forward with the angle of attack increased to 15°. A comparison of Figure 15 with Figure 11 indicates that with

additional wing sweep a vortex can be stabilized on the outer panel by blowing from the fuselage.

On the windward side, ahead of the trailing-edge flap, at 18° angle of attack there is a region of reversed flow evident with the blowing off. At the lowest blowing rate the flow is chordwise again. Dye from the lower surface is pulled to the upper surface near the apex of the leeward wing by the blowing. At the highest blowing rate, a vortex begins to form ahead of the jet and aft of the knee of the leading-edge flap near mid-semispan of the leeward wing at 18° angle of attack. A vortex is still present on the leeward, outboard wing panel, but it bursts farther forward.

With the lowest blowing rate, a weak vortex forms on the leeward wing at 20° angle of attack. By increasing the blowing to the highest rate, the vortex becomes concentrated and has increased rotational velocity. Most of the vortex is aft of the flap hinge line, but farther inboard the vortex is above the flap. The vortex on the outboard wing panel at 20° angle of attack is burst shortly after it forms. This vortex is becoming diffuse and unsteady.

As the angle of attack is increased from 20° to 25°, a vortex begins to form on the windward wing panel when the highest blowing rate of C_μ = 0.06/0.06 is applied. With the leading-edge flap deflected 30° and with the effective sweep reduced on the windward side, a higher angle of attack is required for the windward wing vortex to form. At 25° angle

of attack, a weak vortex appears ahead of the jet on the windward side for the lowest blowing rate. On the windward side at the highest blowing rate, dye is pulled to the upper surface from under the wing, and the wing vortex can now be seen. Part of the vortex is above the flap, and part is aft of the hinge line. On the leeward side at 25° angle of attack, the vortex forms close to the leading edge, and its path is mainly above the leading-edge flap. The flow reattachment aft of the leeward vortex is evident in the smooth, chordwise surface flow downstream of the vortex. It becomes difficult to see the leeward vortex in Figure 15 near mid-semispan of the wing when the large mass flow from the jet begins to mix with the vortex. No vortex was formed at 25° angle of attack on the outboard wing panel.

With no blowing at 30° angle of attack, both wings are stalled except for a small area on the leading-edge flap near the apex. There is now a large region of low velocity and even reversed flow above the stalled wings. Above both wings there is an induced outboard, spanwise flow. On the windward wing the flow direction is no longer toward the fuselage centerline as was the case at low angles of attack. This "adverse" sidewash at high angles of attack is felt at the vertical tail along with a reduction in the dynamic pressure. These effects combine to cause the loss of vertical tail effectiveness and directional stability that has been measured on an F-4 model in Reference 13.

The lowest blowing rate has little beneficial effect on the flow field at 30° angle of attack, as can be seen in Figure 15. A wing vortex was not formed on either side. Very little of the flow ahead of the trailing-edge flap is entrained into the jet. At the highest blowing rate of C_μ = 0.06/0.06, vortices are formed on both wings. On the windward side the vortex is farther inboard, and it forms just ahead of the jet. On the leeward side the vortex is much closer to the leading edge. The flow separates at the leading edge and rolls up into the wing vortex. The burst points of both vortices are farther forward relative to their position at 25° angle of attack. The flow on the windward wing ahead of the trailing-edge flap is chordwise at the highest blowing rate. The improved flow field over the trailing-edge flap and above the wing due to spanwise blowing, especially on the windward side, should increase the vertical tail effectiveness and thereby increase the directional stability at high angles of attack. Such an increase in directional stability due to spanwise blowing has been measured on several fighter aircraft models (References 5, 6, and 8).

Spanwise Blowing on Alternate Landing Configuration in Sideslip

The results obtained for the model at 10° of sideslip with flap deflections of δ_n = 0°/30°/30° and δ_f = 60° are presented in Figure 16 for spanwise blowing from nozzles

located at x/c_r = 0.13 and 0.88. With no blowing at 12° angle of attack, a vortex forms on the windward side. With the inboard flap segment at zero deflection there is no longer a delay in the formation of the windward vortex, as there was for the 30° flap deflection presented in Figure 15. The lowest jet momentum coefficients that were tested on this configuration are C_μ = 0.024/0.018. With this blowing rate at 12° angle of attack, the windward vortex is more concentrated. The leeward vortex shifts farther outboard with blowing. This vortex breaks down when it reaches the outer edge of the inboard leading-edge flap segment. At this point there is an abrupt change from the 0° deflection to the 30° deflection of the flap. The feeding sheet to the leading-edge vortex is stopped, and there is some turbulent flow coming through the gap between the flaps. The highest jet momentum coefficients used on this configuration are C_μ = 0.06/0.06. With this blowing rate at 12° angle of attack, a vortex is formed on the outboard, leeward wing panel. This vortex is in a similar location to the vortex seen in Figure 15 at 10° angle of attack. The leeward wing vortex extends beyond the inboard flap at the highest blowing rate. When the jet combines with the vortex, the added mass flow makes it appear more diffuse, but there is still rotational motion after they combine.

The windward vortex is seen in Figure 16 to shift farther inboard in sideslip. The leeward vortex shifts closer to the leading edge of the wing. The leeward vortex breaks down at 15° angle of attack when it reaches the spanwise station of the end of the inboard flap. This vortex burst point is farther forward than at zero sideslip with no blowing, as seen in Figure 13. This early vortex burst could result in a loss of vortex lift and a change in lateral stability.

At 15° angle of attack, a vortex forms ahead of the jet on the windward side for the lowest blowing rate. The leeward vortex is shifted closer to the leading edge at the low blowing rate, and it extends outboard to the discontinuity in the leading-edge flap. A vortex is formed on the leeward, outboard wing panel for the highest blowing rate. It bursts at a location similar to that seen with the inboard flap deflected in Figure 15 at 15° angle of attack. The windward vortex shifts farther outboard with the higher blowing. It breaks down when it reaches the end of the inboard flap. The higher blowing rate enables the leeward vortex to extend beyond the inboard flap segment at 15° angle of attack, where it begins to turn back toward the streamwise direction.

With no blowing at 18° angle of attack, the leeward vortex again breaks down at the end of the inboard flap. This is farther forward than at zero sideslip. The windward vortex shifts far enough inboard in sideslip to remain inboard of the break in the leading-edge flap. The burst point of the wind-

ward vortex moves forward with the increase in the angle of attack from 15° to 18°. The lowest blowing rate has little effect on the burst point of the leeward vortex at 18° angle of attack in Figure 16. The burst point of the leeward vortex is fixed by the spanwise location of the break in the flap. For the highest blowing rate at 18° angle of attack, the leeward vortex does not extend beyond the end of the inboard flap. A vortex is again formed on the leeward, outboard wing panel.

At 20° angle of attack with no blowing, the windward vortex has moved to the apex of the wing and the windward wing is stalled. The leeward wing vortex has greater stability and a slower progression of its burst point at high angles of attack. A vortex is still present on the leeward wing, as seen in Figure 16 at 20° angle of attack. The leeward wing would then be generating greater lift than the windward wing, and a destabilizing rolling moment results. This can cause a loss in effective dihedral, as is discussed in References 13 and 14. In Figure 15 with all three segments of the leading-edge flap deflected 30°, the flap was seen to maintain attached flow near the apex on the leading edge and so delay the stall of the windward wing. It was shown in Reference 13 that a 40° droop in the leading edge of the F-4 would maintain a moderate level of lateral stability to high angles of attack. With the blowing off, the configuration with δ_n = 0°/30°/30° would probably have less lateral stability than with the uniform leading-edge flap deflection of 30°. Deflection of the lead-

ing-edge flaps improves the lateral/directional characteristics of the F-4 over those with no flaps by delaying the leading-edge separation to higher angles of attack. Any favorable increment in lateral or directional stability due to blowing would be reduced when the flaps are deflected. Smaller increments in stability from spanwise blowing were measured on the fighter aircraft of Reference 6 when the leading-edge flaps were deflected. The lateral/directional stability should be more sensitive to blowing for the configuration with the inboard flap segment undeflected.

With the lowest blowing rate at 20° angle of attack, a vortex is formed on the windward wing which was stalled before. On the leeward side it can be seen in Figure 16 that the burst of the leading-edge vortex is delayed to farther outboard by the spanwise blowing. At the highest blowing rate, the vortex could extend farther outboard if it were not for the discontinuity in the flap deflection. In Figure 15 the vortex extends across most of the inboard wing panel at 20° angle of attack with the same blowing rate.

Figure 16 shows that the leeward wing is stalled by 25° angle of attack with no blowing. Both wings are now stalled. For the lowest blowing rate, a vortex is formed on both the leeward and windward wings. The improved flow field over the trailing-edge flap and above the wing due to spanwise blowing should increase the vertical tail effectiveness and thereby increase the directional stability at high angles of attack for

this configuration. The higher blowing rate shows little shift in the wing vortex burst locations when compared to the lowest blowing rate. At 30° angle of attack, the separated flow above both wings with no blowing is illustrated in Figure 16. At the lowest blowing rate, the burst point of the leeward vortex moves forward when the angle of attack is increased from 25° to 30°. This vortex burst occurs inboard of the end of the inboard flap segment. With the highest blowing rate, the burst points for both vortices are again delayed to near the end of the inboard flaps. There appears to be little difference from the flow field seen at 25° angle of attack in Figure 16.

Spanwise Blowing Over Outboard Wing in Maneuver Configuration

The tests of the model in sideslip, illustrated in Figures 15 and 16, showed that on the leeward side, a vortex could be stabilized on the outboard wing panel with blowing from the fuselage. To stabilize this vortex at zero sideslip, when the wing is at a lower effective leading-edge sweep angle, would require a higher blowing rate. When the spanwise blowing is from the fuselage, the jet undergoes considerable spreading and is turned rearward by the crossflow before it reaches the outboard wing panel. If the nozzle were located at the outer edge of the inboard wing panel, instead of at the fuselage, the outboard vortex could be stabilized using a lower

jet momentum coefficient. A lower jet momentum coefficient could be provided up to higher velocities in flight. This would extend the utility of spanwise blowing into the maneuver flight regime rather than being effective only under landing conditions. Applying spanwise blowing on the outboard wing panel would replace the turbulent wake with a leading-edge vortex and reattached flow. It may then be possible to reduce the severity of both transonic buffet and high angle of attack wing rock.

To study the application of spanwise blowing to maneuvering flight, the flaps were changed from their landing configuration. The three segments of the leading-edge flap were set to 15°, while the trailing-edge flap was also deflected 15°. The flap setting of δ_n/δ_f = 15°/15° is representative of a maneuver flap setting of a fighter aircraft. A nozzle position study was conducted for the outboard nozzle to determine the importance of chordwise location and nozzle sweep angle. The spanwise location for the nozzles was at the wing hinge line between the inboard and outboard wing panels. The chordwise nozzle locations tested were 25% and 35% of the chord of the inboard wing panel at the wing hinge. The nozzle was set both parallel to the leading edge and at a sweep angle of 10° less than the leading-edge sweep of the outboard wing panel. Details of the nozzle size and positions are given in Table 1.

The effects of blowing from the four outboard nozzle positions are illustrated in Figure 17. The comparison of the nozzle positions is made at 18° angle of attack for jet momentum coefficients of 0.01 and 0.03, based on wing area. The first nozzle position presented in Figure 17 is x/c_h = 0.25 and Λ_N = 53.6°. At the lowest blowing rate of 0.01, a leading-edge vortex is formed ahead of the jet, but it breaks down before reaching the trailing edge. At the highest blowing rate of 0.03, the leading-edge vortex extends across the span of the outboard wing panel to near the wing tip, where it curves aft and coalesces with the wing-tip vortex. This wing-tip vortex extends to aft of the horizontal tail. The second nozzle position presented in Figure 17 is x/c_h = 0.35 and Λ_N = 53.6°. For the lower blowing rate of 0.01 there is no vortex formed on the outer wing panel. The nozzle is too far aft for the feeding sheet from the leading edge to form a vortex in the low pressure region just ahead of the jet. The flow which separates at the leading edge is well above the surface as it moves aft over the nozzle. With the higher blowing rate, a vortex is seen ahead of the jet, but it was unsteady and burst before reaching the trailing edge. A concentrated tip vortex as seen for the first nozzle position was not found.

The remaining two nozzle positions presented in Figure 17 have nozzle sweep angles of 10° less than the leading-edge sweep angle. The third nozzle position is then Λ_N = 43.6° and x/c_h = 0.25. With the lower blowing rate, a leading-edge

vortex forms and passes over the top of the blowing jet. The vortex breaks down before reaching the trailing edge and no tip vortex is seen. At the highest blowing rate, a vortex rolls up ahead of the jet. Farther outboard the jet expands to the leading edge and beyond the wing tip, and the vortex becomes very diffuse. There is still some rotation in the flow but not the concentrated tip vortex that was seen with the nozzle parallel to the leading edge. The fourth and final nozzle position presented in Figure 17 is $\Lambda_N = 43.6°$ and $x/c_h = 0.35$. At the lowest blowing rate of 0.01, no vortex forms on the outer wing panel. The jet is again too far aft of the leading edge for a vortex to be stabilized ahead of it. At the highest blowing rate, a vortex appears ahead of the jet, but it is unsteady and diffuse.

Spanwise blowing from the first nozzle position of Figure 17, $x/c_h = 0.25$ and $\Lambda_N = 53.6°$, was more effective in stabilizing a vortex over the outboard wing panel for a low blowing rate, and in enhancing the vortex at a high blowing rate. The effects of spanwise blowing from this nozzle position are illustrated in Figure 18 for a range of blowing rates and angles of attack. At 15° angle of attack a vortex has begun to form over the inboard wing panel as the flow separates near the flap hinge line. No vortex flow can be seen on the outboard wing panel. With a blowing rate of only 0.005, a vortex was formed at 15° angle of attack, and it extends across the outboard wing panel. Near the wing tip the vortex

curves streamwise and combines with the wing-tip vortex. At a blowing rate of 0.01, the vortex above the outboard wing panel appeared to be stronger, and the tip vortex was more concentrated and could be seen to extend beyond the horizontal tail. Increasing the blowing rate to the highest level of 0.03 appears to produce a diffuse vortex due to more of the jet mass flow being entrained into the vortex. The problems of excessive jet velocity and entrainment of fluid into the vortex are discussed in greater detail in Reference 15.

A strong vortex is seen on the inboard wing panel at 18° angle of attack for the blowing off case in Figure 18. The secondary vortex can also be seen between the wing leading edge and the primary vortex. At 18° angle of attack, the blowing rate of 0.005 is not sufficient to form a stable vortex on the outboard wing panel. A vortex is formed at C_μ = 0.01, but it breaks down before reaching the trailing edge. It is not until the highest blowing rate tested, 0.03, that the vortex above the outboard panel and at the wing tip is seen.

Increasing the angle of attack to 20° with no blowing causes the inboard vortex to burst farther forward and inboard. A vortex is not seen on the outboard wing panel in Figure 18 at 20° angle of attack until the highest blowing rate. No tip vortex is seen as the leading-edge vortex was unsteady, and it bursts ahead of the trailing edge. Although there was no outboard vortex at C_μ = 0.01, there is a considerable delay in the breakdown of the inboard vortex. The location of the

vortex burst is close to that seen at 18° angle of attack in Figure 18. The outboard spanwise blowing jet is entraining flow which could induce greater spanwise flow over the inboard wing panel. The breakdown of the inboard vortex is also delayed with the highest blowing rate. At 25° angle of attack, the inboard wing panel vortex is completely broken down. The inboard vortex did not reform for any of the outboard blowing rates tested. A vortex is seen on the outboard wing panel at 25° angle of attack for only the highest blowing rate tested, 0.03. The vortex extends from the apex of the snag to just aft of the exit of the nozzle.

Spanwise Blowing Over Inboard and Outboard Wing Panels in Maneuver Configuration

With spanwise blowing applied to both the inboard and the outboard wing panels, the flow over most of the span of the wing could be controlled. Delaying the breakdown of both the inboard and the outboard vortex to higher angles of attack would significantly increase the vortex lift and thereby improve the maneuver performance provided the engine bleed requirements are kept low. The outboard nozzle position of x/c_h = 0.25 and Λ_N = 53.6°, which was shown in Figure 17 to be the most effective, was used. The inboard nozzle at the wing fuselage junction was positioned at x/c_r= 0.13 and Λ_N = 51.4°. This forward nozzle position is more effective with

zero or small leading-edge flap deflections while a farther aft position of x/c_r = 0.30 was seen in Figures 6 and 7 to be the most effective with a large flap deflection. The flap deflections for the maneuver configuration are δ_n/δ_f = 15°/15°.

For the lowest blowing rates of C_μ = 0.01/0.01, a vortex is seen on the outboard wing panel at 15° angle of attack in Figure 20. This vortex appears to be the same as that seen in Figure 18 for outboard blowing alone. At the highest blowing rate of C_μ = 0.03/0.03, the outboard vortex again becomes diffuse. Over the inboard wing panel a vortex is beginning to form just aft of the flap hinge line and ahead of the jet at 15° angle of attack.

At 18° angle of attack, there is little change in the outboard vortex at the lowest blowing rate from that seen with outboard blowing alone in Figure 18. At the highest blowing rate, however, the inboard blowing does help produce a more concentrated outboard vortex. The burst point of the inboard vortex is seen to be delayed to farther outboard with spanwise blowing. The secondary vortex can be a seen for the lowest blowing rate at 18° angle of attack. The path of the inboard vortex is shifted to one of lesser sweep when the inboard spanwise blowing is applied.

The spanwise blowing over the inboard wing panel at 20° angle of attack is seen in Figure 19 to be able to delay the vortex breakdown to only sightly farther outboard than the outboard blowing alone did in Figure 18. Blowing from both the

inboard and outboard nozzles has a synergistic effect. The outboard blowing is seen in Figure 18 to delay the breakdown of the inboard vortex at 20° angle of attack. At the highest blowing rate, the inboard blowing is seen in Figure 19 to help form a more concentrated and steady outboard vortex at 20° angle of attack.

An inboard vortex was formed at 25° angle of attack with the lowest blowing rate from the inboard nozzle. No inboard vortex was seen with the blowing off or with outboard blowing alone in Figure 18. A vortex is seen in Figure 19 on the outboard wing panel at 25° angle of attack for only the highest blowing rate tested, 0.03/0.03. The vortex extends from the apex of the snag to just aft of the exit of the nozzle.

The effects of spanwise blowing from nozzles located at x/c_r = 0.13 and outboard at x/c_h = 0.25 for the model at 10° of sideslip with flap deflections of δ_n/δ_f = 15°/15° are illustrated in Figure 20. The outboard spanwise blowing enables a vortex to form at 15° angle of attack on both the leeward and windward outboard wing panels. The inboard blowing jet causes the leeward, inboard vortex to shift closer to the leading edge. Increasing the inboard blowing rate from 0.01 to 0.03 further enhanced the leeward vortex and delayed the vortex breakdown to farther aft and outboard. A weak, inboard vortex is formed on the windward side at the lowest blowing rate. At the higher blowing rate, the dye on the windward side is entrained directly into the jet and the vortex is not visible.

The inboard, windward vortex is seen ahead of the jet at the lowest blowing rate at 18° angle of attack, but at the highest blowing rate there is again no dye reaching the windward vortex. The inboard blowing on the windward side turns the flow ahead of the trailing-edge flap from spanwise to more chordwise. The blowing rate of 0.01/0.01 is not sufficient at 18° angle of attack to form an outboard vortex on the windward side. The leading-edge sweep is effectively reduced on the windward side in sideslip. On the leeward side a vortex is formed at the low blowing rate but it bursts before reaching the trailing edge. The higher blowing rate is required to form the outboard, windward vortex. For C_μ = 0.03/0.03, this vortex is formed, but it breaks down near the wing tip at 18° angle of attack. On the leeward side, the vortex turns and coalesces with the wing-tip vortex.

At 20° angle of attack, the outboard vortices are formed only at the highest blowing rate. The vortex which forms on the leeward side has greater stability and it bursts farther aft than the windward vortex, as seen in Figure 20. The inboard blowing is able to delay the bursting of both the windward and the leeward vortices to farther aft and outboard at the lowest blowing rate of 0.01/0.01. Increasing the blowing rate increases both the apparent strength and the stability of the vortices as seen in the increased rotational velocity and the farther outboard delay of the vortex breakdown. At the higher blowing rate, the jet is able to expand

farther spanwise before being turned by the crossflow. This moves the path of the vortices closer to the leading edge of the wing.

The inboard vortex is completely broken down with the blowing off at 25° angle of attack on both the windward and leeward sides. With spanwise blowing from the inboard nozzles, a weak vortex forms on the windward side which breaks down farther forward than the vortex seen in Figure 19 at zero sideslip and 25° angle of attack. On the leeward side, with its greater effective wing sweep, a more concentrated vortex is formed than on the windward side. At 25° angle of attack, a vortex is seen in Figure 20 on the outboard wing panels at only the highest blowing rate of 0.03/0.03 and only on the leeward side.

CONCLUDING REMARKS

Flow visualization studies were conducted in the Northrop water tunnel to provide a qualitative evaluation of the benefits of spanwise blowing applied to the F-4. Details of the changes that occur in the vortex flow fields above the wing due to spanwise blowing were obtained for angles of attack from 10° to 30° at sideslip angles of 0° to 10°. The sensitivity of the vortex flows to changes in flap deflection angle, nozzle position, and jet momentum coefficient was determined. A

summary of the flow visualization results is given below and conclusions are made where appropriate:

1. Spanwise blowing from the fuselage over the inboard wing panel was found to delay the breakdown of the wing vortex to farther outboard and to higher angles of attack. Increasing the blowing rate at a constant angle of attack enhanced the vortex, increasing its apparent strength. With increasing blowing rate, the blowing jet expands farther forward and extends farther outward. This helps in delaying the vortex burst to farther outboard and can shift the path of the vortex outward. Increasing the angle of attack requires an increased blowing rate to form a stable vortex at a given spanwise station. Spanwise blowing produces smooth, chordwise flow over the trailing edge which can improve the trailing-edge flap effectiveness.
2. With a leading-edge flap deflection of 30°, the most effective spanwise blowing location was aft of the flap hinge line. The vortex first formed when flow separation occurred at the knee of the flap. Deflection of the leading-edge flap delays flow separation, thereby delaying the formation of the wing vortex to higher angles of attack. This then delays the lift increase generatd by spanwise

blowing to enhance the wing vortex to a higher angle of attack.

3. Spanwise blowing over the trailing-edge flap entrains flow downward, which produces a lift increase over a wide range of angles of attack. This blowing changes the flow direction ahead of the flap from spanwise to more chordwise. At 25° angle of attack, the trailing-edge flap blowing delayed the burst of the vortex above the inboard wing panel.
4. An undeflected inboard flap segment allows the leading-edge vortex to form at a lower angle of attack. The lift enhancement from blowing to stabilize the leading-edge vortex will then begin at a lower angle of attack. This would be beneficial in landing because greater lift is produced at a lower and more useful angle of attack. Leaving the inboard flap segment undeflected did, however, limit the spanwise extent of the leading-edge vortex. With spanwise blowing, the wing vortex would extend farther outboard if the discontinuity in the flap deflection were shifted outboard.
5. The higher effective sweep angle of the windward wing in sideslip increases the stability of the vortex and thereby delays the burst. The reduced effective sweep angle of the leeward wing decreases the vortex stability, and the vortex bursts farther

inboard. When the wing sweep is reduced, a higher blowing rate is required to maintain a stable vortex. Spanwise blowing delays the stall of the windward wing to higher angles of attack by delaying the burst of the windward wing vortex. This would help to maintain vertical tail effectiveness and the directional stability to higher angles of attack.

6. A vortex can be stabilized on the outboard wing panel at a lower blowing rate using an outboard nozzle. The most effective nozzle position tested was with the nozzle at 25% of the local chord and swept parallel to the leading edge. Blowing from both an inboard and an outboard nozzle was seen to have a favorable interaction. The inboard blowing helps to enhance the outboard vortex. The outboard blowing delays the burst of the inboard vortex.

REFERENCES

1. Dixon, C.J., "Lift Augmentation by Lateral Blowing Over a Lifting Surface," AIAA Paper 69-193, Feb. 1969.
2. Bradley, R.G., Wray, W.O., and Smith, C.W., "An Experimental Investigation of Leading-Edge Vortex Augmentation by Blowing," NASA CR-132415, 1974.
3. Bradley, R. G., Whitten, P. D., and Wray, W. O., "Leading-Edge Vortex Augmentation in Compressible Flow," AIAA Paper 75-124, Jan. 1975.
4. Campbell, J. F., "Effects of Spanwise Blowing on the Pressure Field and Vortex-Lift Characteristics of a 44° Swept Trapezoidal Wing," NASA TN D-7907, 1975.
5. Erickson, G. E. and Campbell, J. F., "Improvement of Maneuver Aerodynamics by Spanwise Blowing," NASA TP-1065, 1977.
6. Erickson, G.E., "Effect of Spanwise Blowing on the Aerodynamic Characteristics of the F-5E," AIAA Paper 79-0118, Jan. 1979.
7. Scruggs, R. M. and Theisen, J. G., "Transonic Buffet Response Testing and Control," Unsteady Aerodynamics, Volume I, Proceedings of a Symposium, Univeristy of Arizona, March 1975.

8. Anglin, E. L. and Satran, D., "Effects of Spanwise Blowing on Two Fighter Airplane Configurations," AIAA Paper 79-1663, Aug. 1979.

9. Dixon, C.J., "Lift and Control Augmentation by Spanwiuse Blowing Over Trailing Edge Flaps and Control Surfaces," AIAA Paper 72-781, Aug. 1972.

10. Erickson, G., "Water Tunnel Flow Visualization: Insight Into Complex Three-Dimensional Flow Fields," AIAA Paper 79-1530, July 1979.

11. Poisson-Quinton, Ph. and Werlé, H., "Water Tunnel Visualization of Vortex Flow," Astronautics and Aeronautics, June 1967.

12. Werlé, H., "Hydrodynamics Flow Visualization," Annual Review of Fluid Mechanics, Volume 5, pp. 361-382, 1973.

13. Chambers, J. R. and Anglin, E. L., "Analysis of Lateral-Directional Stability Characteristics of a Twin-Jet Fighter Airplane at High Angles of Attack," NASA TN D-5361, 1969.

14. Lorincz, D. J., "Water Tunnel Flow Visualization Study of the F-15," NASA CR-144878, Dec. 1978.

15. Theisen, J. G., Scruggs, R. M., and Dixon, C. J., "Theoretical and Experimental Investigations of Vortex Lift Control by Spanwise Blowing," Volume II, LG73ER-0169, Lockheed-Georgia Co., Sept. 1973.

TABLE I. NOZZLE GEOMETRY AND POSITION

NOZZLE LOCATION	x/c	Λ_N deg	DIAMETER cm	h/d
Inboard	0.13	51.4	0.17	1.33
Inboard	0.30	51.4	0.17	1.33
Trailing-Edge Flap	0.88	17.0	0.12	1.0
Outboard	0.25	53.6	0.08	1.0
Outboard	0.25	43.6	0.08	1.0
Outboard	0.35	53.6	0.08	1.0
Outboard	0.35	43.6	0.08	1.0

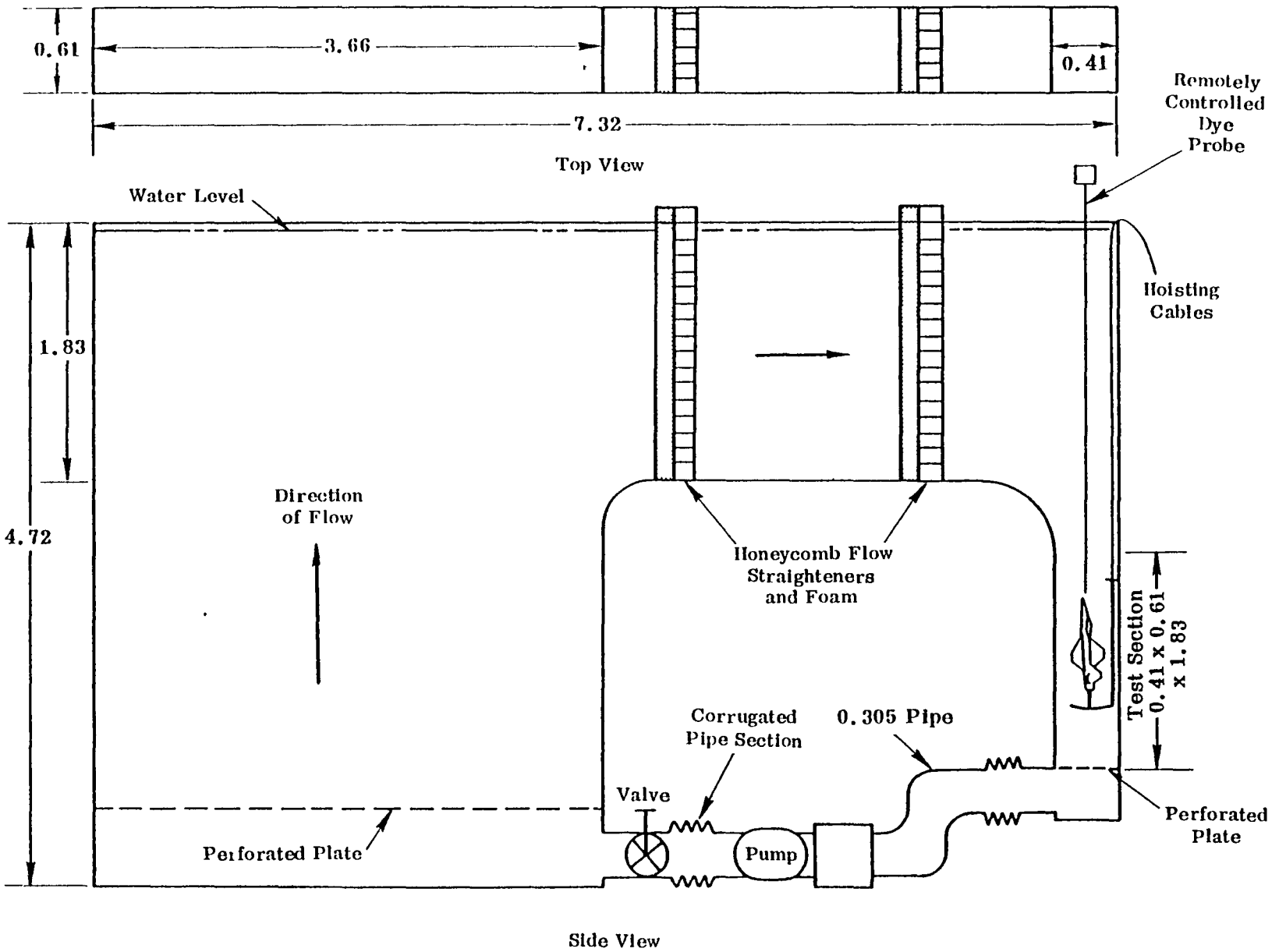

FIGURE 1. NORTHROP DIAGNOSTIC WATER TUNNEL (ALL DIMENSIONS IN M)

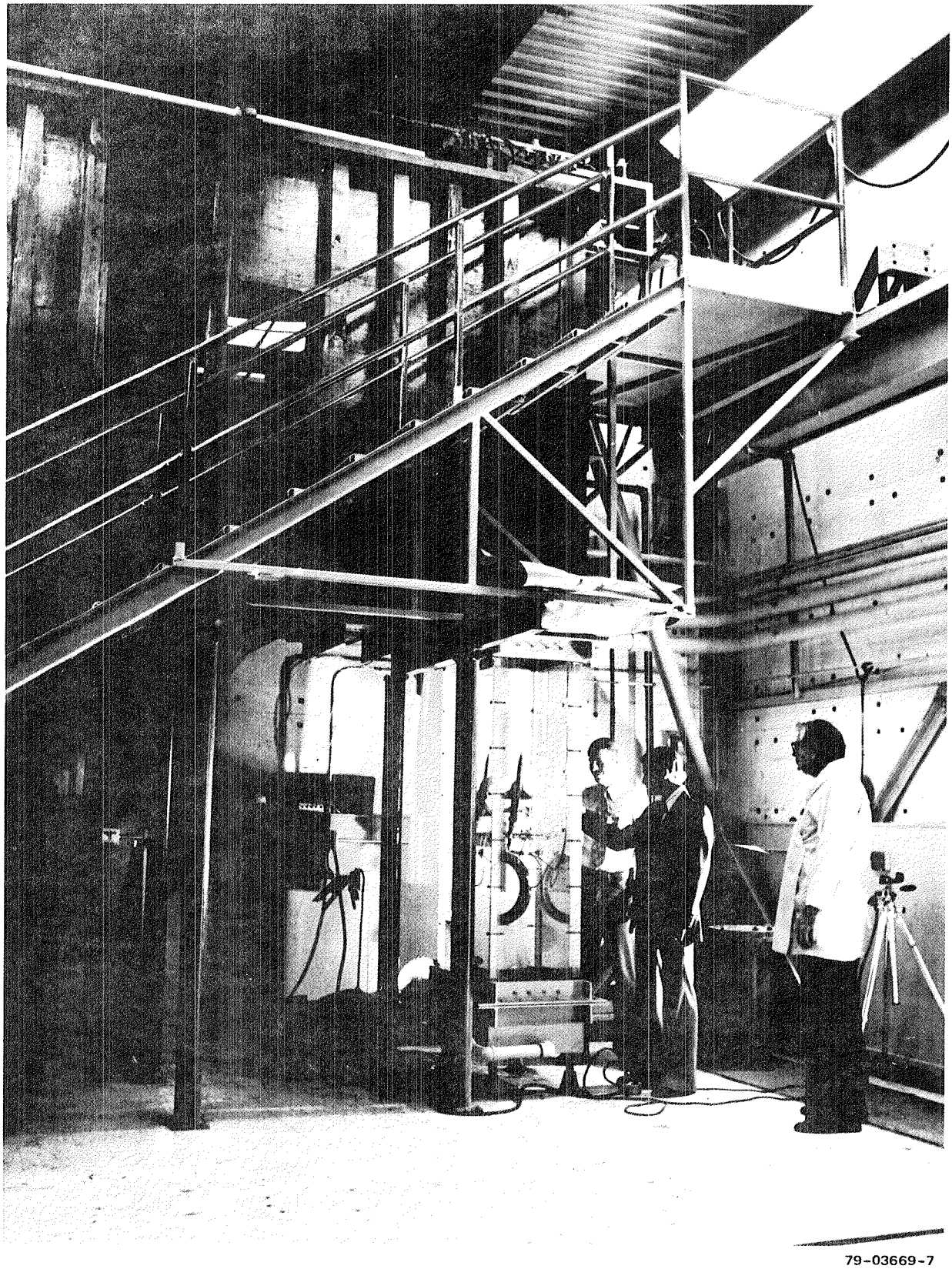

79-03669-7

FIGURE 2. MODEL INSTALLED IN WATER TUNNEL

		Facility (Method)	Reynolds No.
○	Northrop 16 x 24 in.	Water Tunnel (Dye)	$2.0(10^4)$
●	Northrop 6 x 6 in.	Water Tunnel (Dye)	$1.5(10^4)$
□	Wentz	Wind Tunnel (Schlieren)	10^6 (approx.)
◇	Poisson-Quinton & Erlich	Water Tank (Dye; aluminum Particles)	$2(10^4)$ (approx.)
△	Chigier	Wind Tunnel (Laser anemometer)	$2(10^6)$ (approx.)
▽	Earnshaw and Lawford	Wind Tunnel (Tuft probe)	(10^6) (approx.)
▲	Hummel and Srinivasan	Wind Tunnel (Smoke)	(10^6) (approx.)
☆	Lowson	Water Tunnel (Dye)	$3(10^4)$

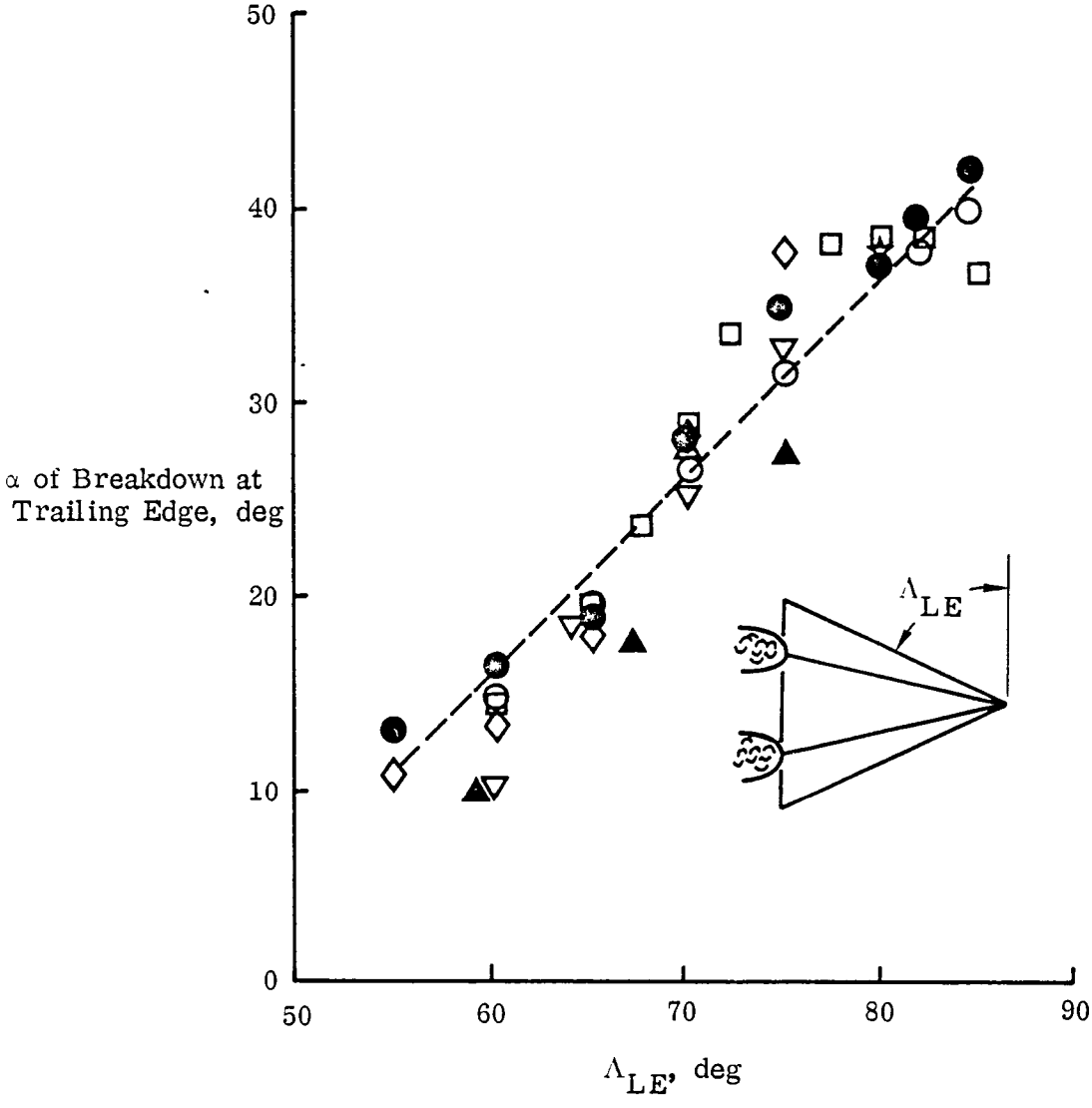

FIGURE 3. EFFECT OF LEADING-EDGE SWEEP ON THE ANGLE OF ATTACK OF VORTEX BREAKDOWN AT THE TRAILING EDGE OF DELTA WINGS (DATA FROM REFERENCE 10)

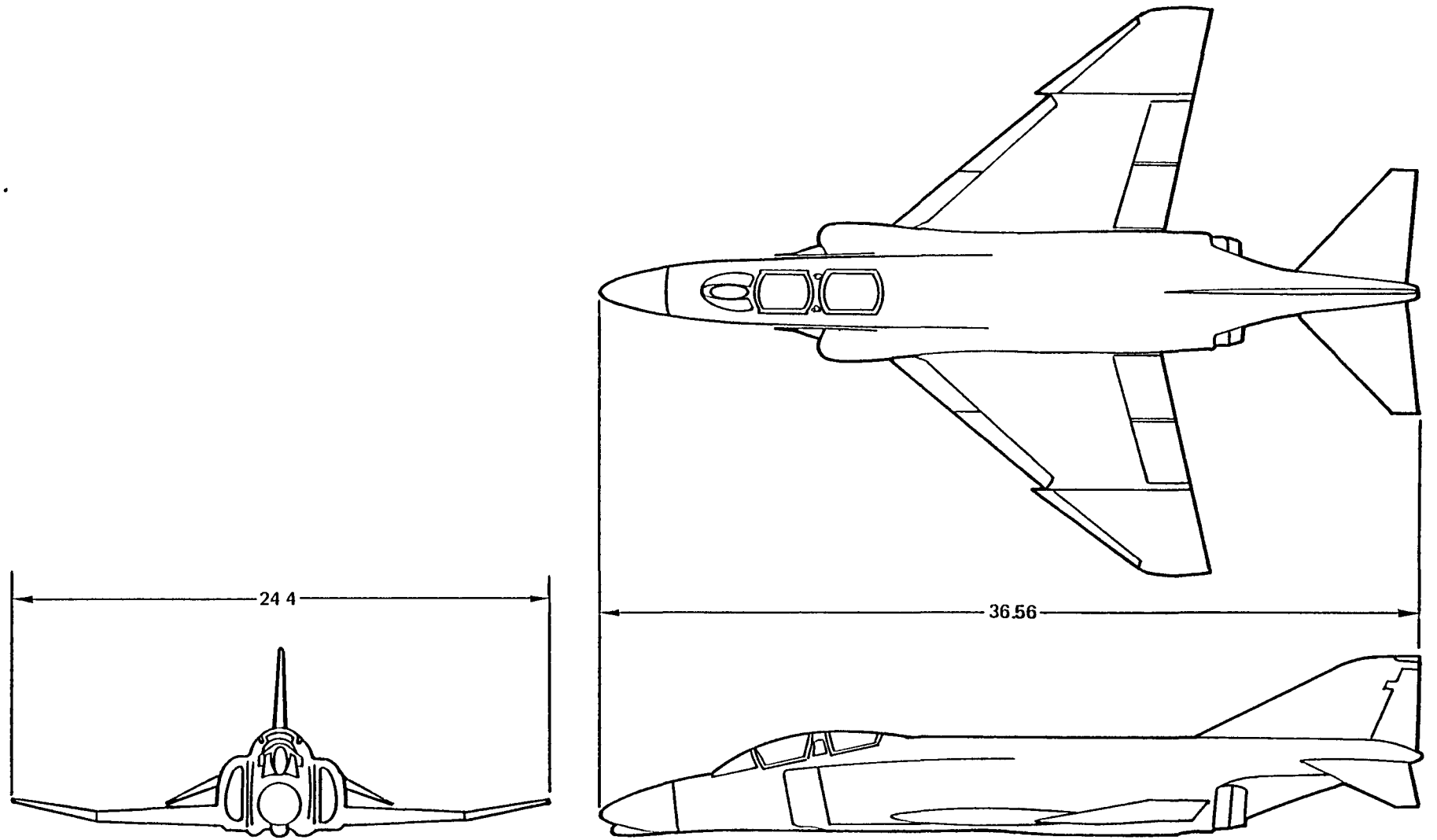

FIGURE 4. 1/48-SCALE F-4 MODEL THREE-VIEW DRAWING (ALL DIMENSIONS IN CM)

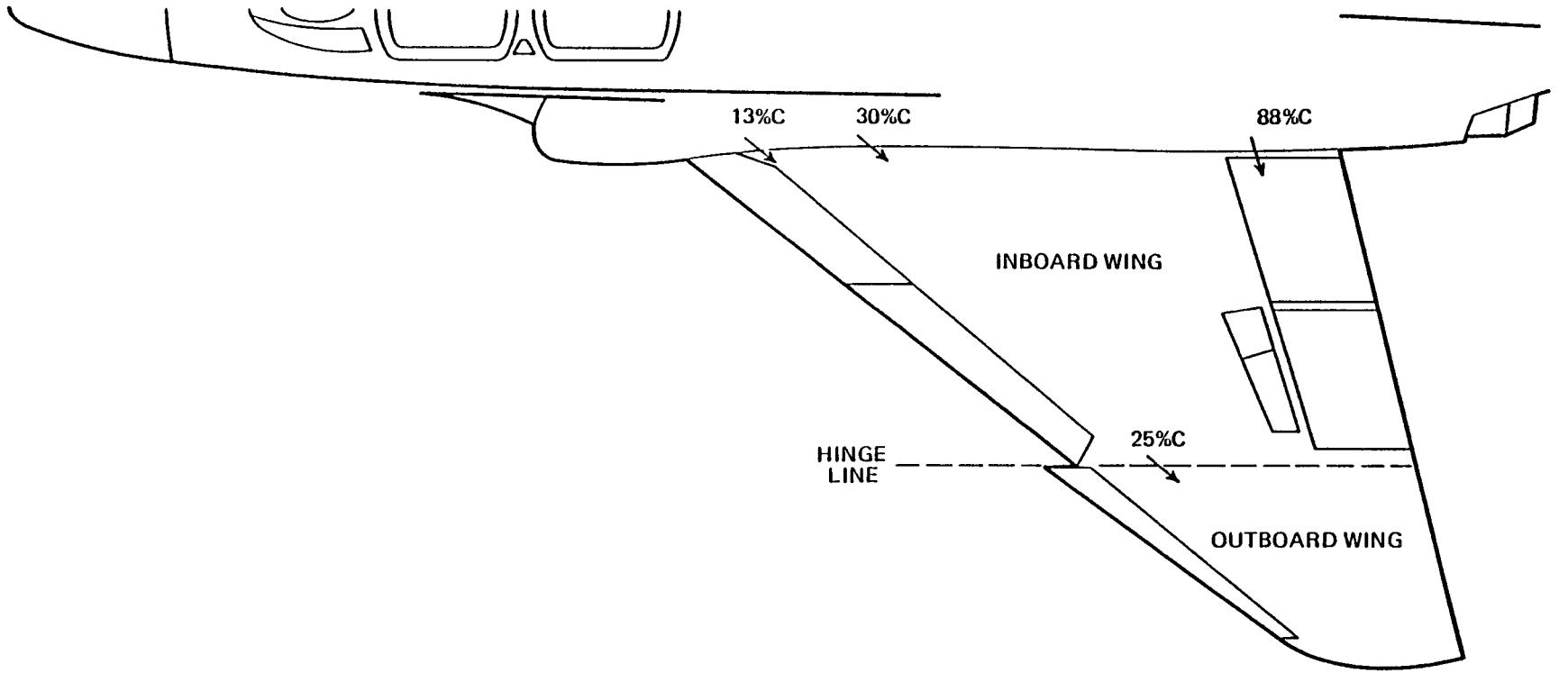

FIGURE 5. NOZZLE POSITIONS

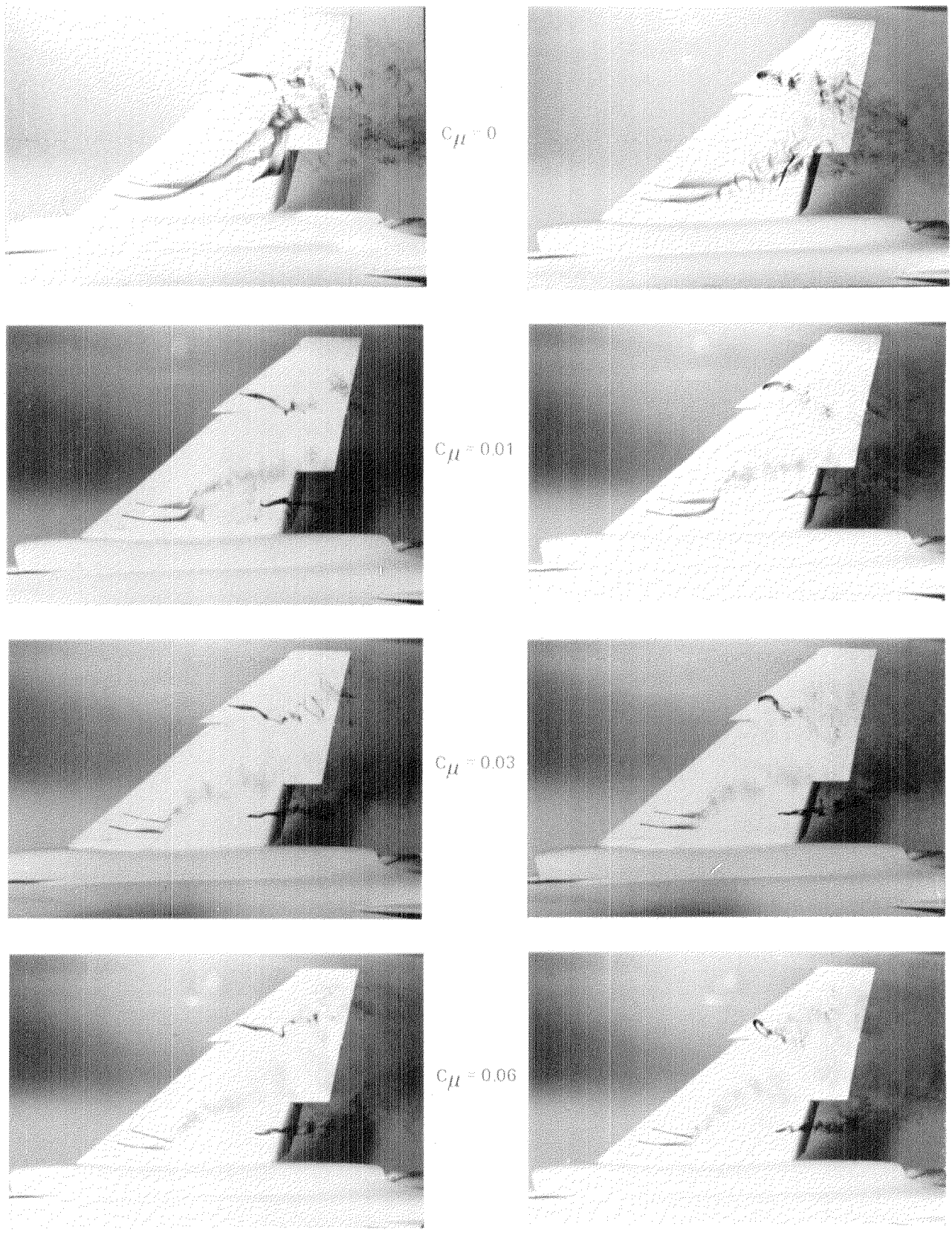

FIGURE 6. SPANWISE BLOWING OVER THE WING FOR $x/c_r = 0.3$, $\delta_n/\delta_f = 30^o/60^o$

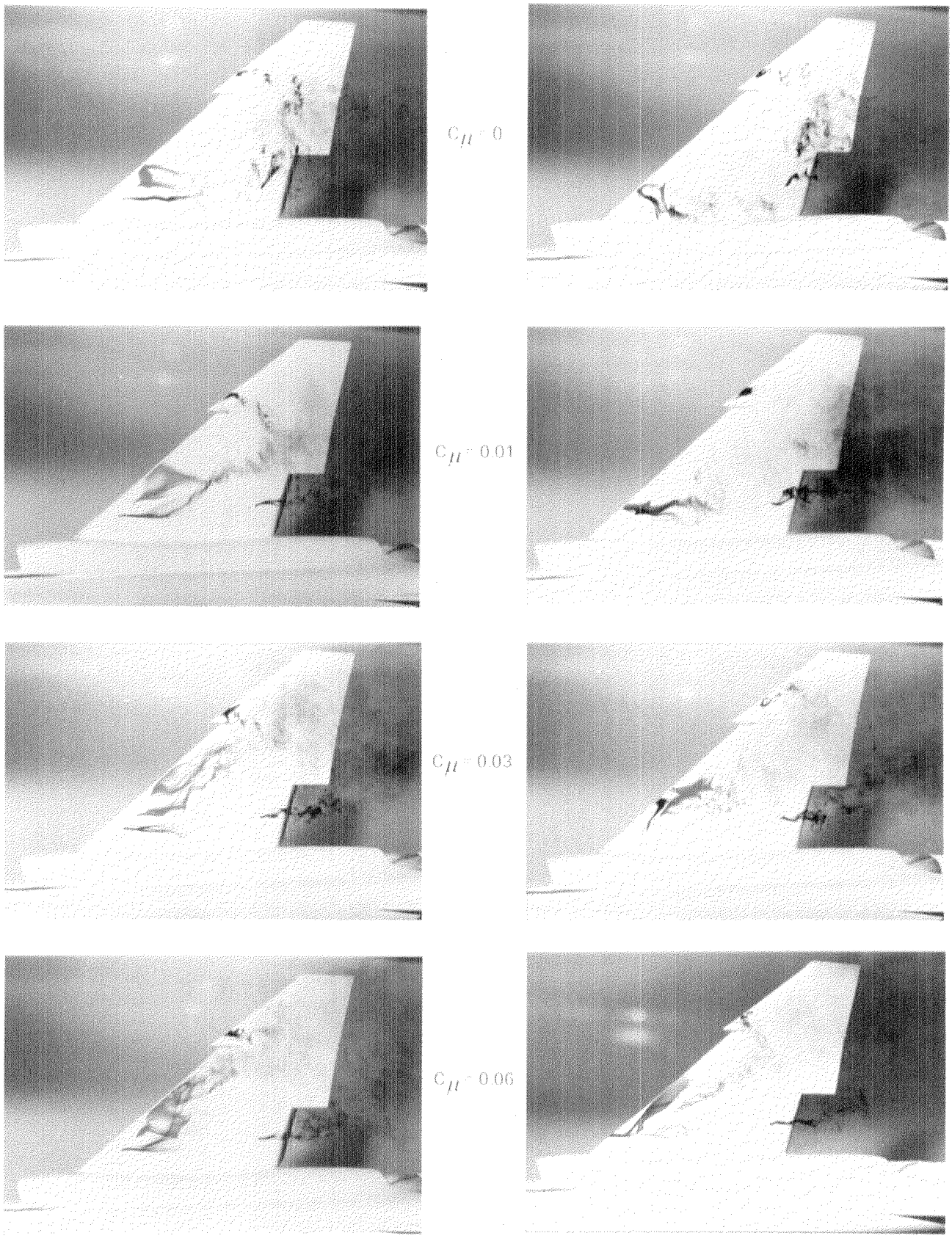

FIGURE 6. CONCLUDED

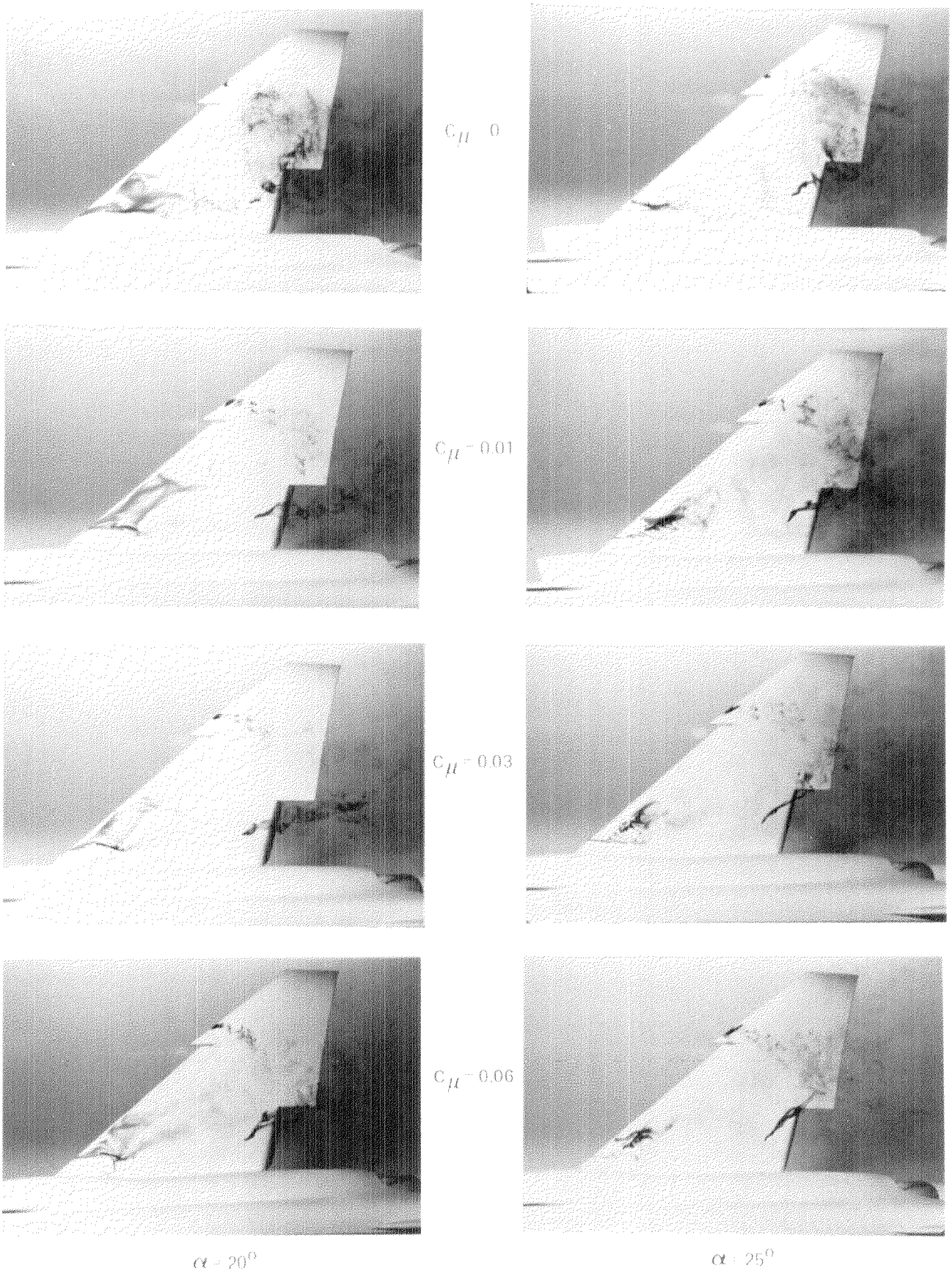

FIGURE 7. SPANWISE BLOWING OVER THE WING FOR $x/c_r = 0.13$, $\delta_n/\delta_f = 30^o/60^o$

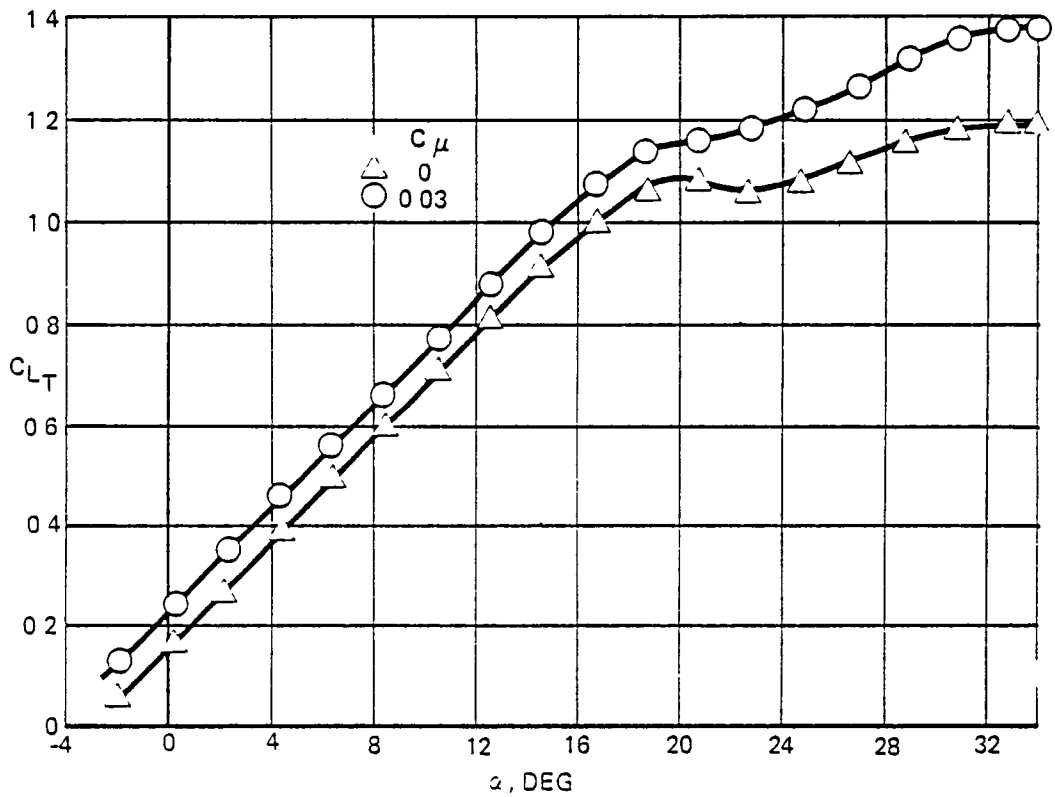

FIGURE 8. EFFECT OF SPANWISE BLOWING OVER WING ON TRIMMED LIFT COEFFICIENTS WITH δ_η = 30°/60°/60°, δ_f = 45°

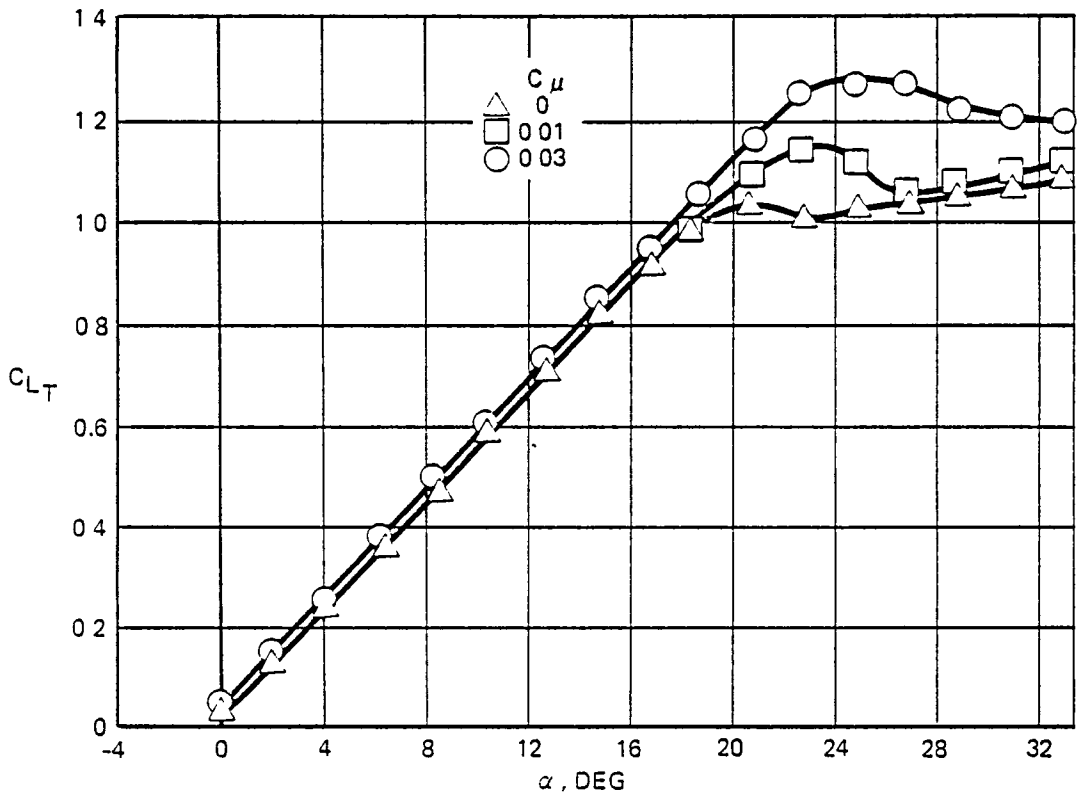

FIGURE 9. EFFECT OF SPANWISE BLOWING OVER WING ON TRIMMED LIFT COEFFICIENTS WITH $\delta_\eta/\delta_f = 0^o/0^o$

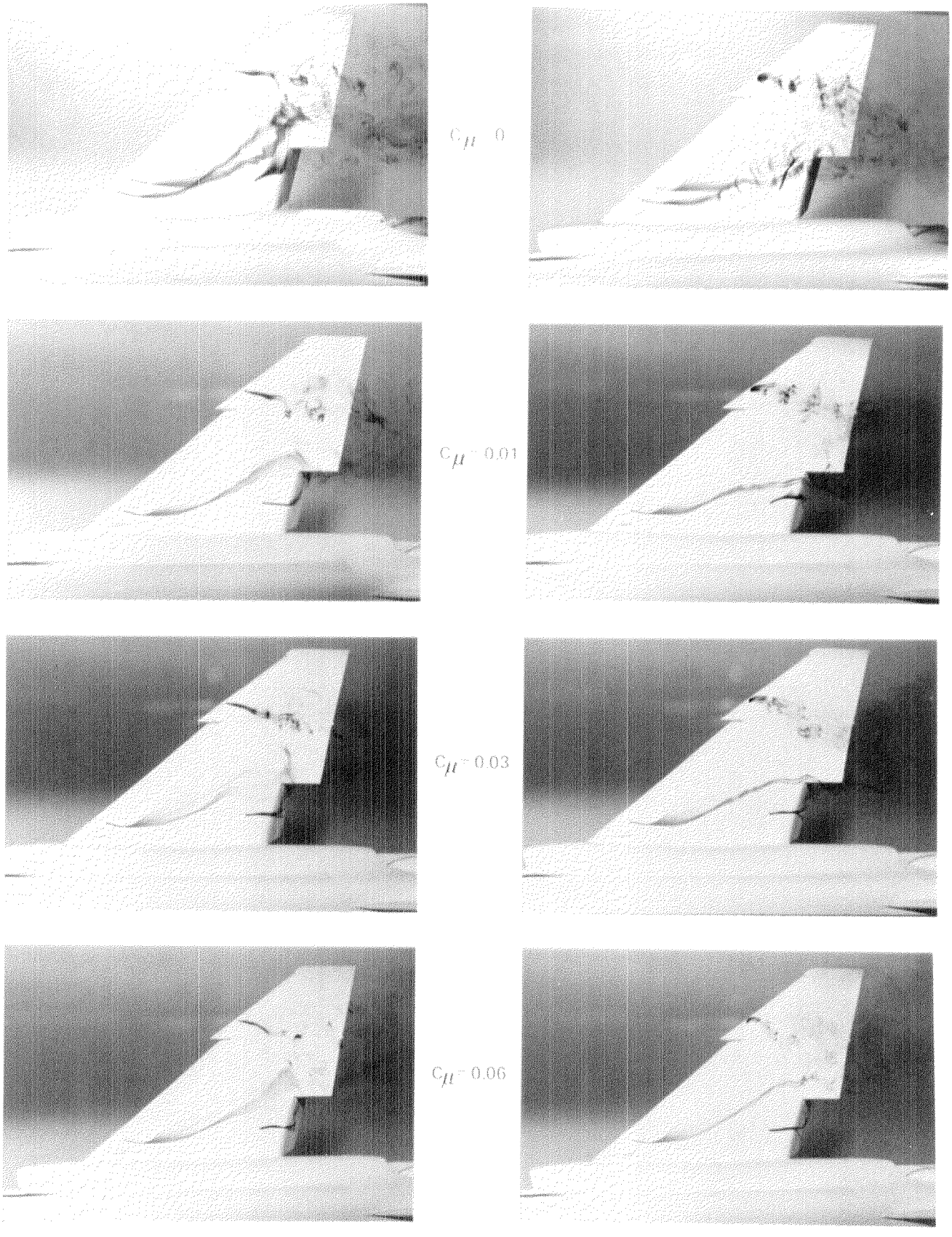

FIGURE 10. SPANWISE BLOWING OVER THE TRAILING-EDGE FLAP FOR $x/c_f = 0.88$, $\delta_n/\delta_f = 30^\circ/60^\circ$

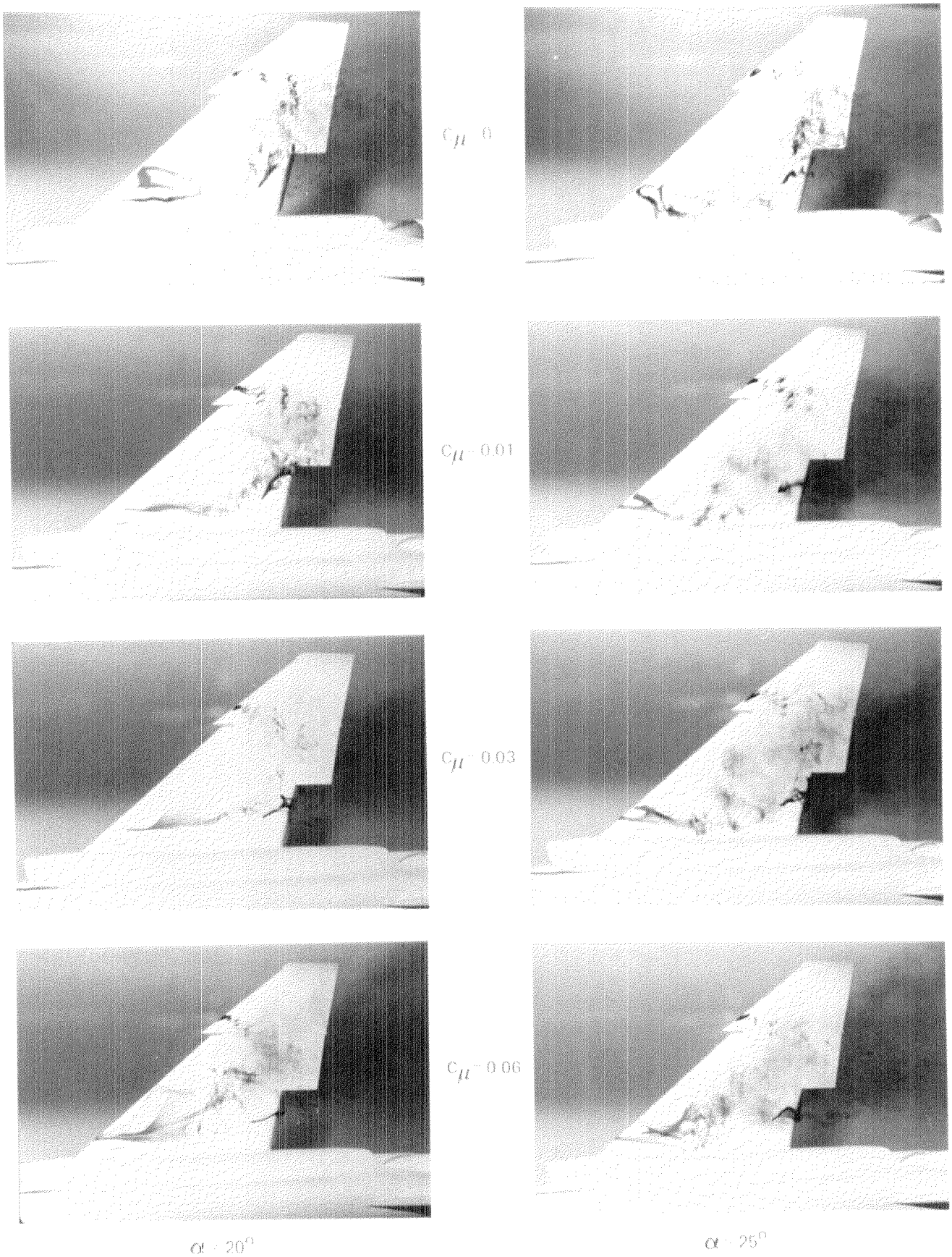

FIGURE 10. CONCLUDED

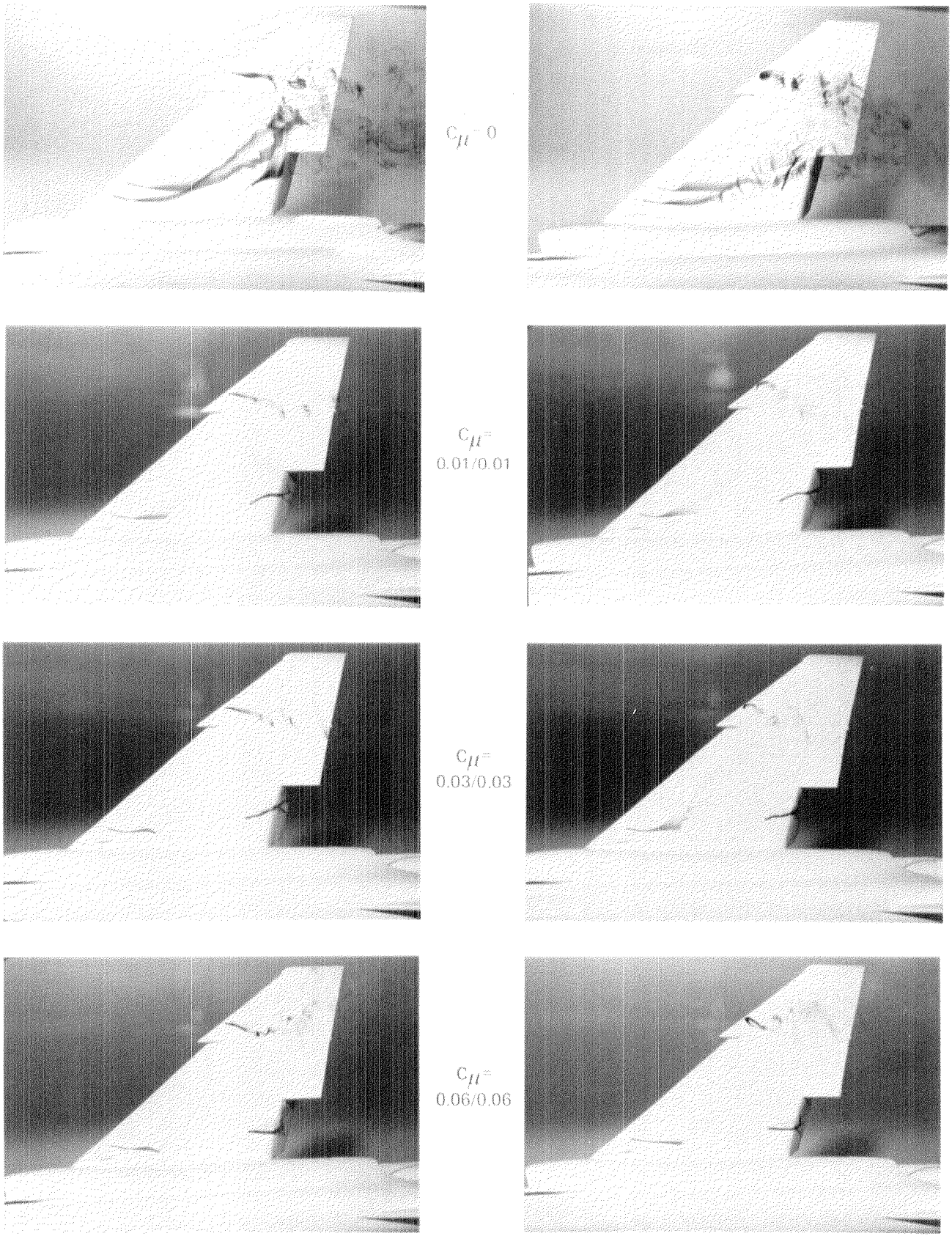

FIGURE 11. SPANWISE BLOWING OVER THE WING AND TRAILING-EDGE FLAP FOR $x/c_r = 0.3$ AND 0.88, $\delta_n/\delta_f = 30^o/60^o$

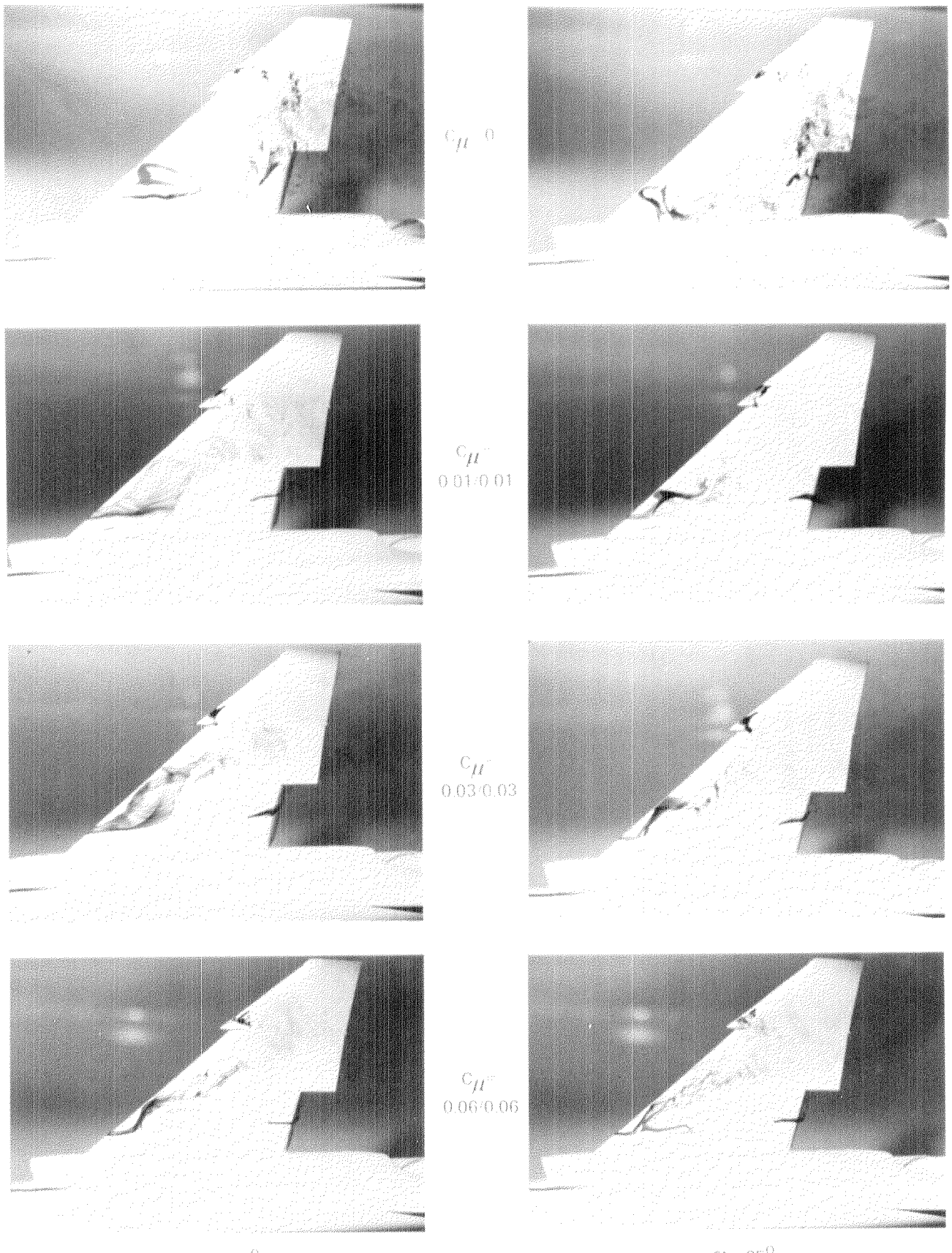

FIGURE 11. CONCLUDED

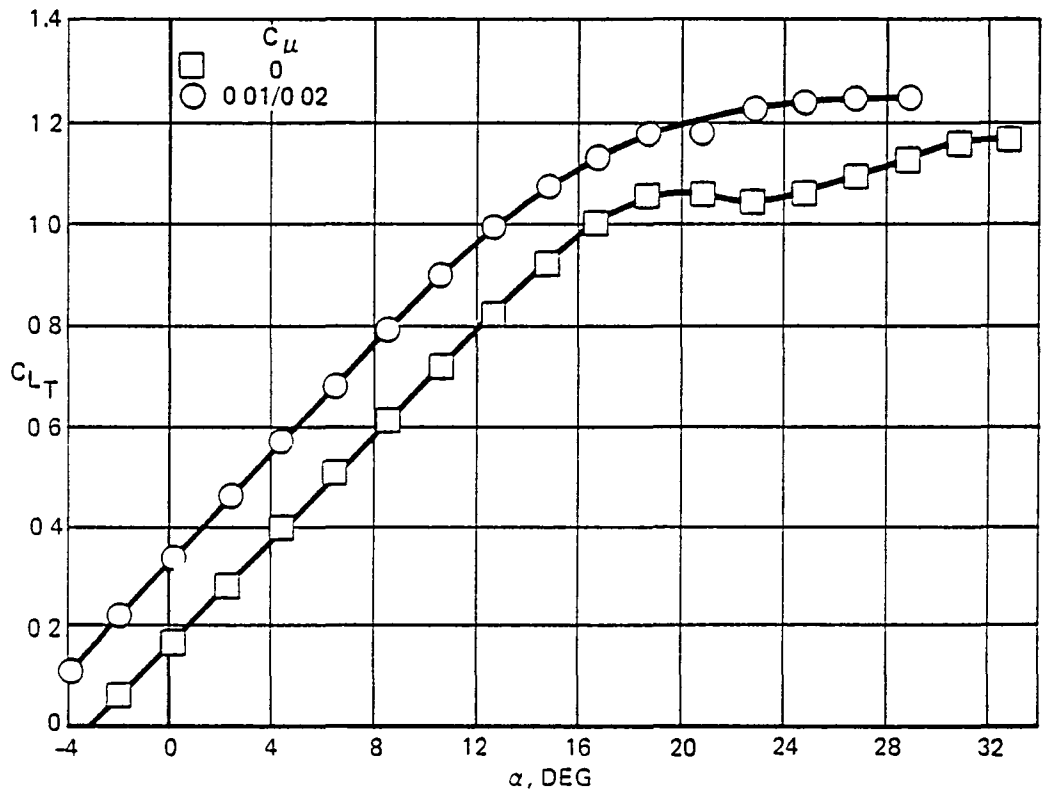

FIGURE 12. EFFECT OF SPANWISE BLOWING OVER WING AND TRAILING -EDGE FLAP ON TRIMMED LIFT COEFFICIENTS WITH δ_η = 20°/60°/60°, δ_f = 60°

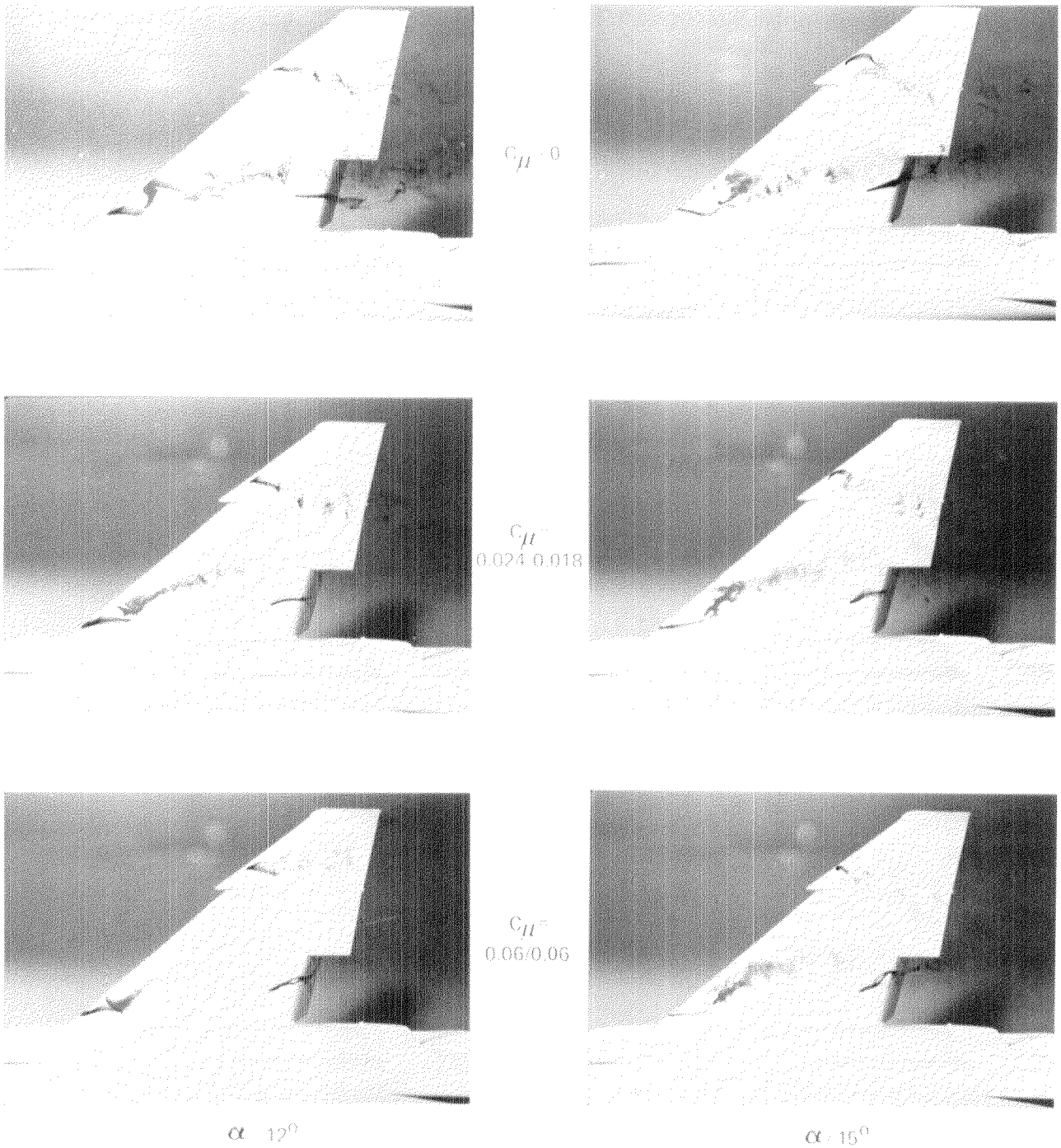

FIGURE 13. SPANWISE BLOWING OVER THE WING AND TRAILING-EDGE FLAP FOR x/c_r = 0.13 AND 0.88, $\delta_n = 0^o/30^o/30^o$, $\delta_f = 60^o$

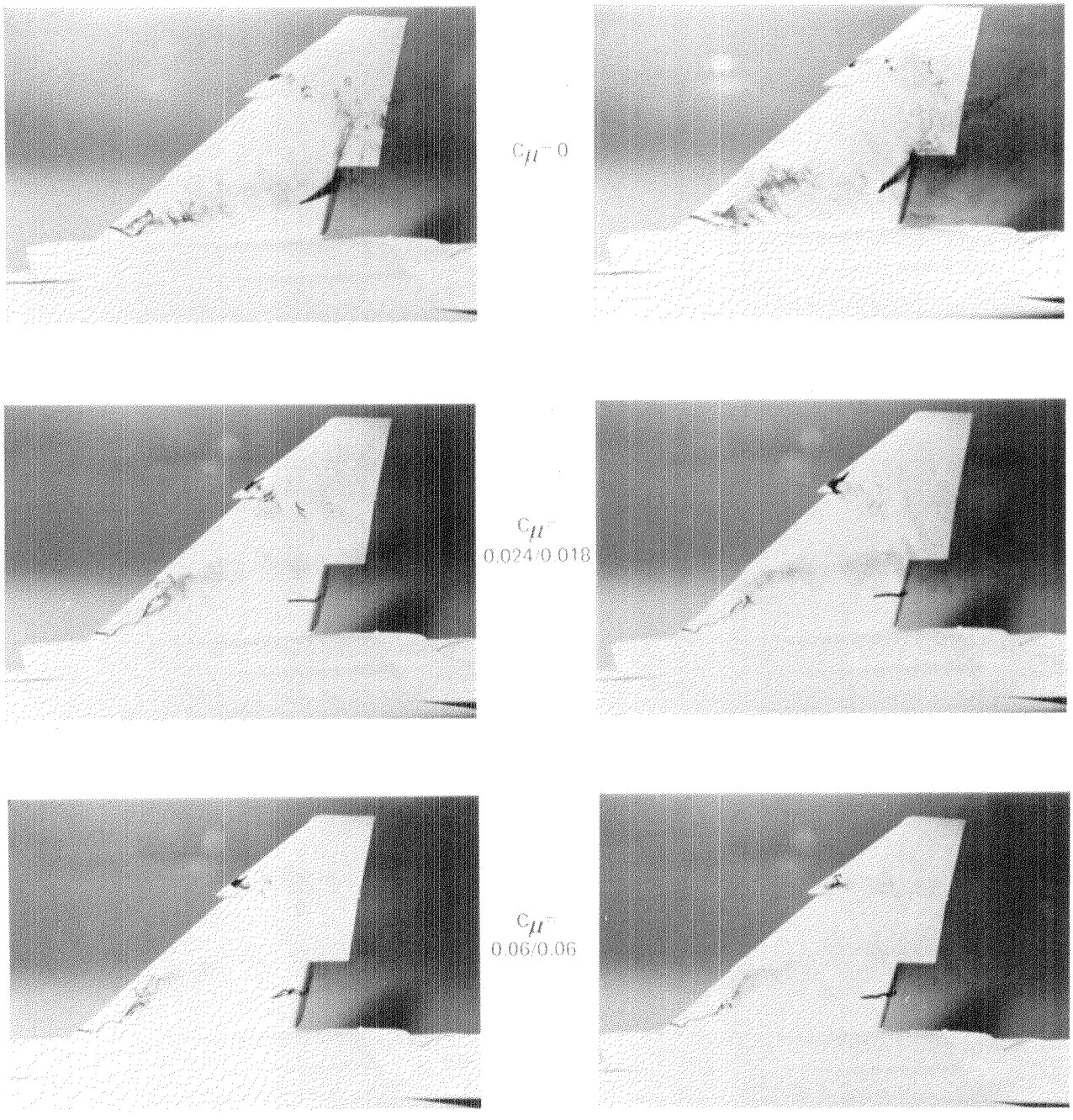

FIGURE 13. CONCLUDED

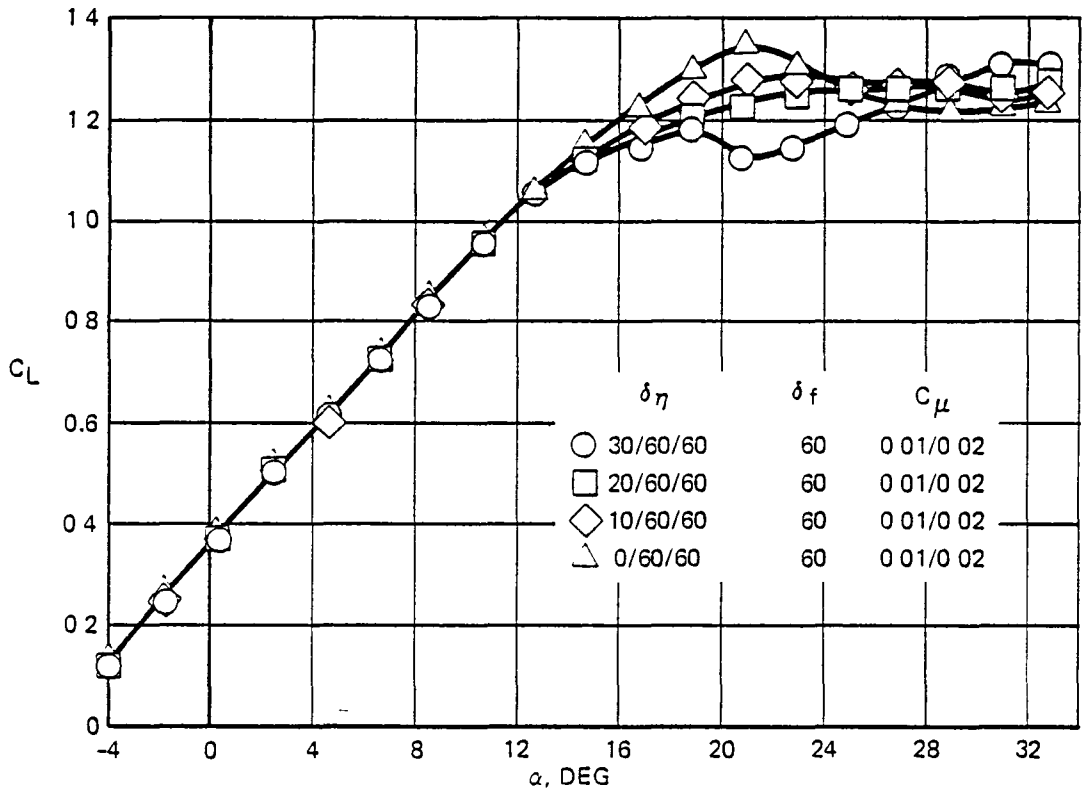

FIGURE 14. EFFECT OF LEADING-EDGE FLAP DEFLECTION ON LIFT CHARACTERISTICS WITH SPANWISE BLOWING OVER WING AND TRAILING-EDGE FLAP

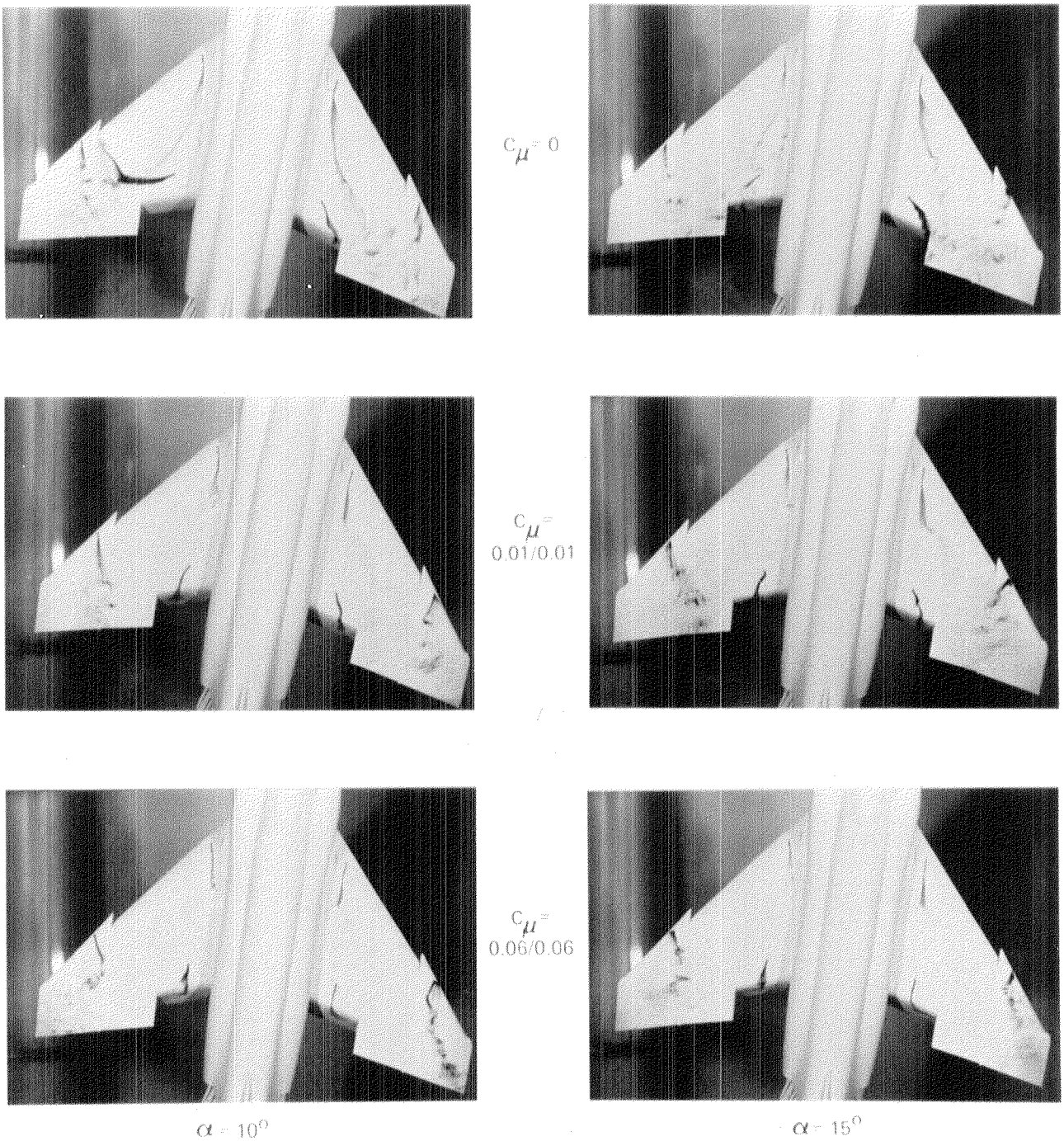

FIGURE 15. SPANWISE BLOWING OVER THE WING AND TRAILING-EDGE FLAP IN SIDESLIP WITH $x/c_r = 0.3$ AND 0.88, $\delta_n/\delta_f = 30^o/60^o, \beta = -10^o$

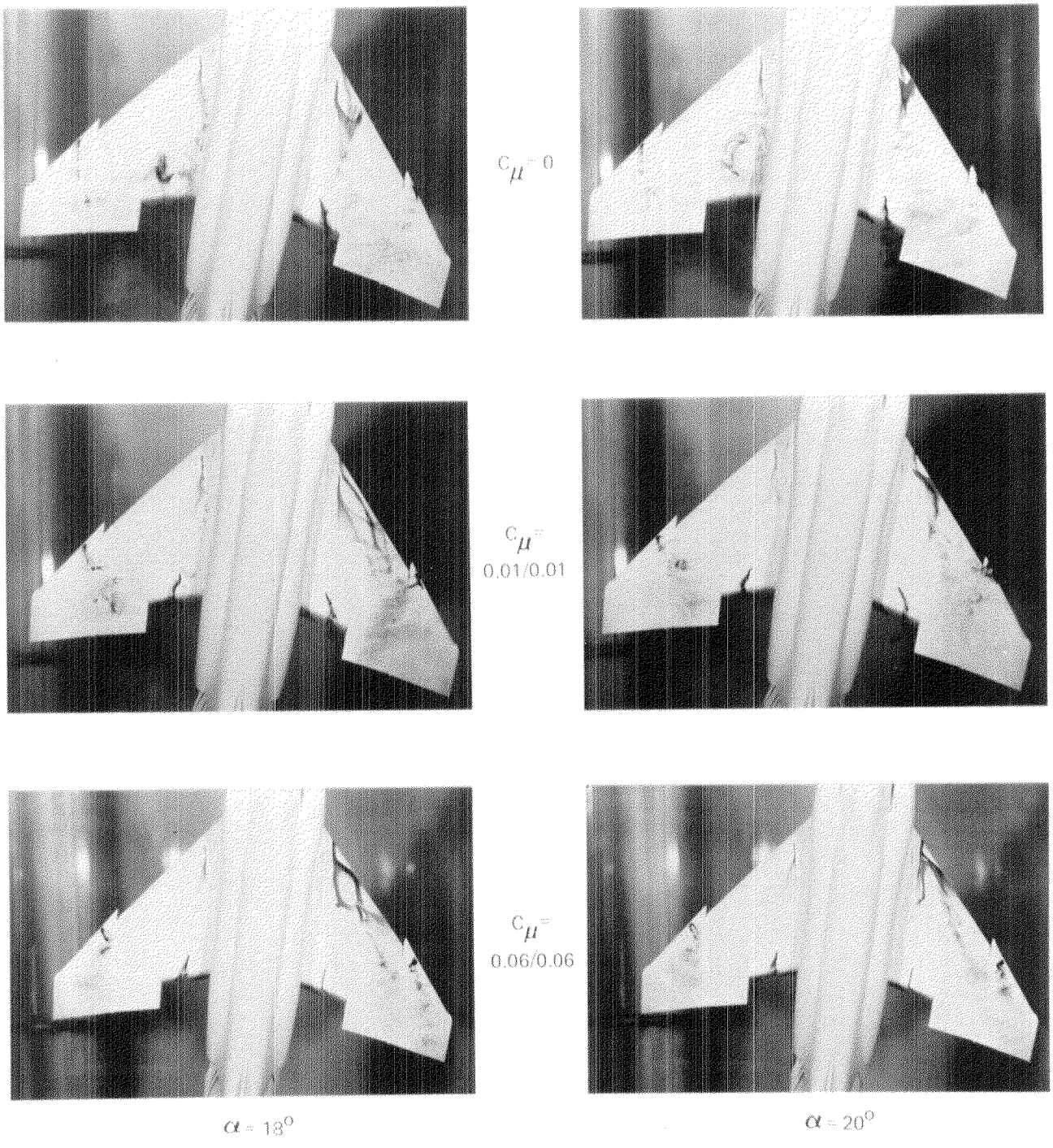

FIGURE 15. CONTINUED

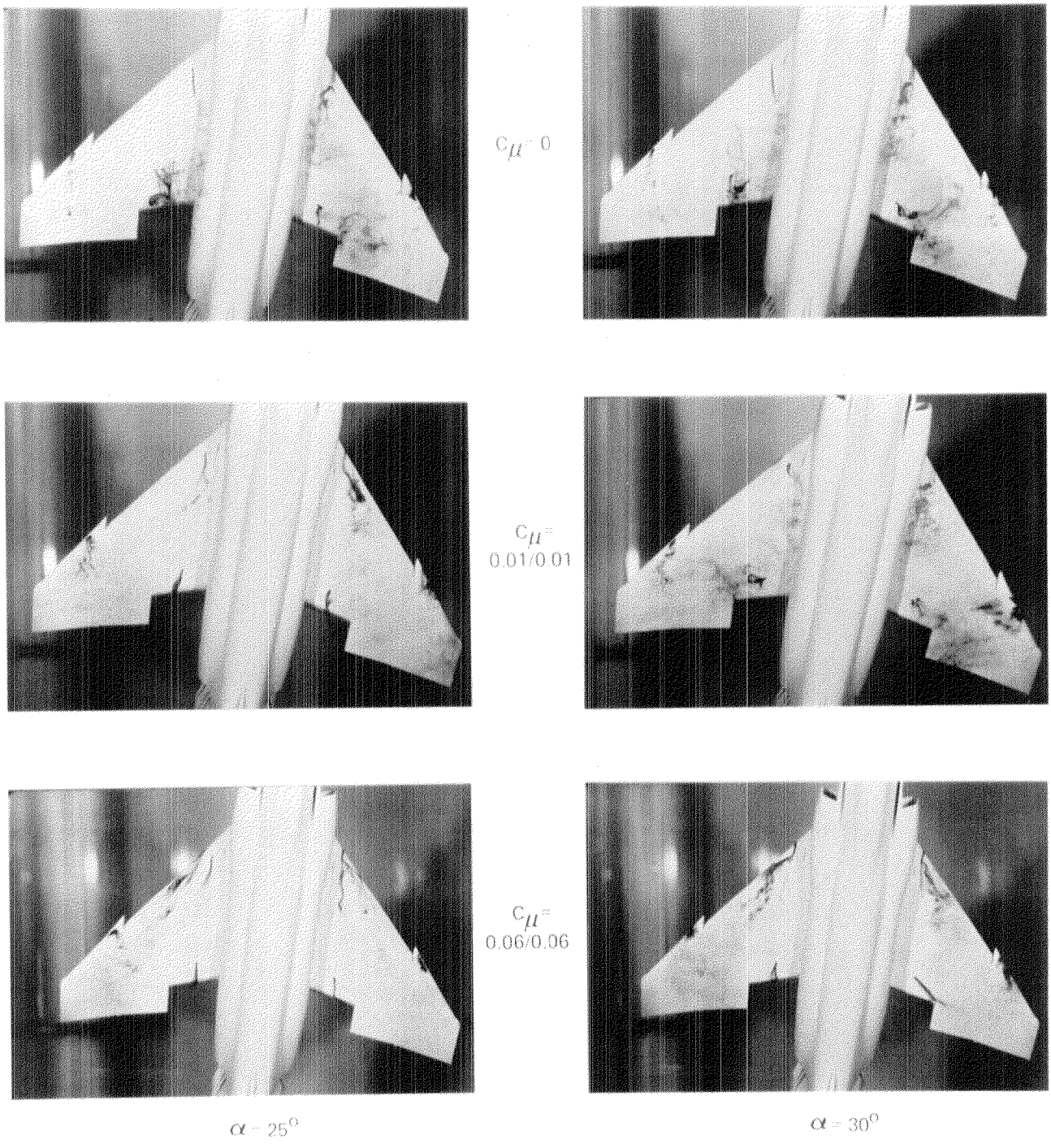

FIGURE 15. CONCLUDED

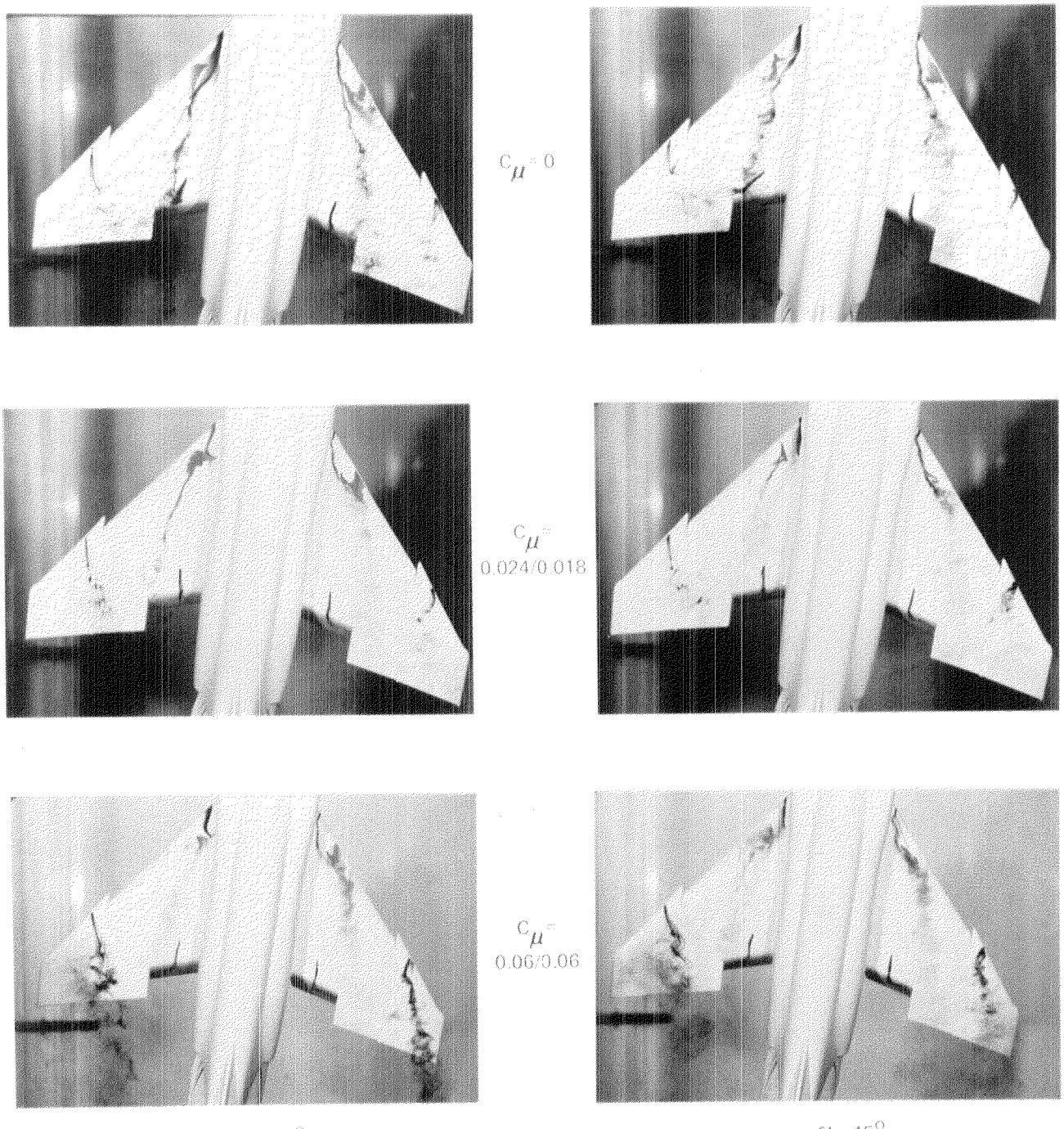

FIGURE 16. SPANWISE BLOWING OVER THE WING AND TRAILING-EDGE FLAP IN SIDESLIP WITH x/c_r = 0.13 AND 0.88, $\delta_n = 0^o/30^o/30^o$, $\delta_f = 60^o$, $\beta = -10^o$

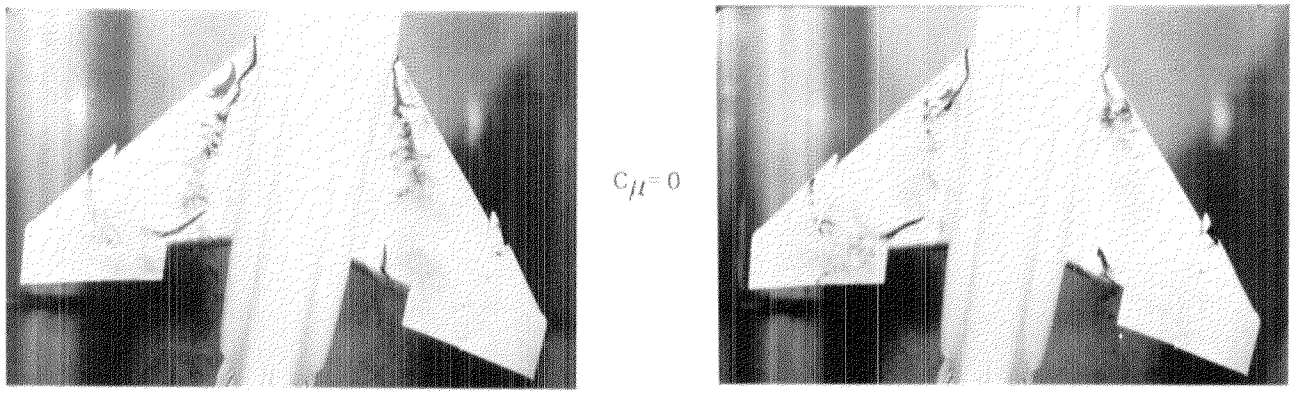

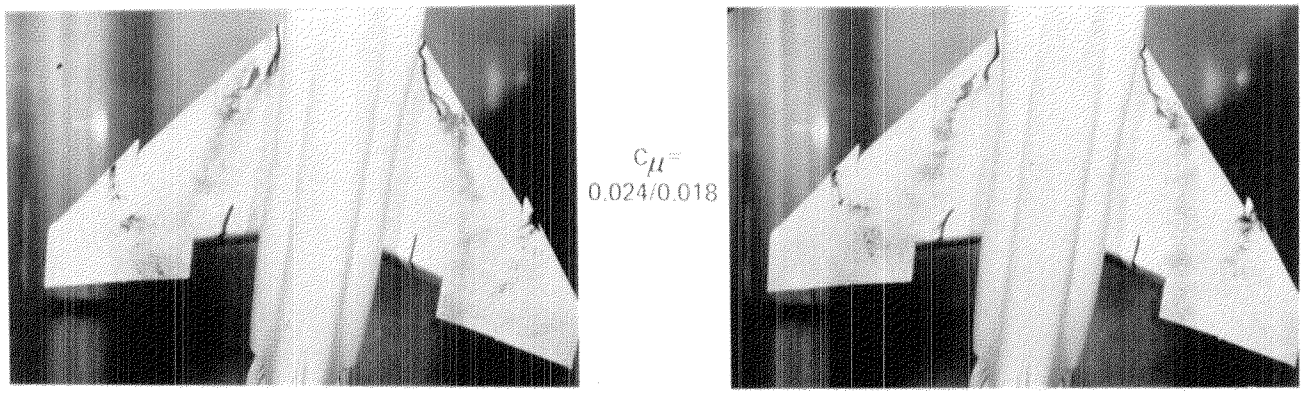

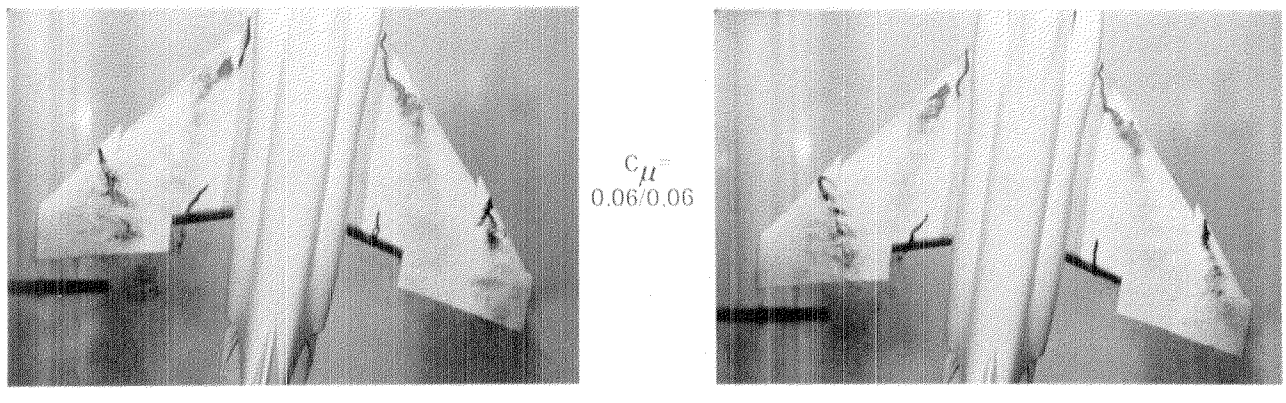

$\alpha = 18^\circ$ $\alpha = 20^\circ$

FIGURE 16. CONTINUED

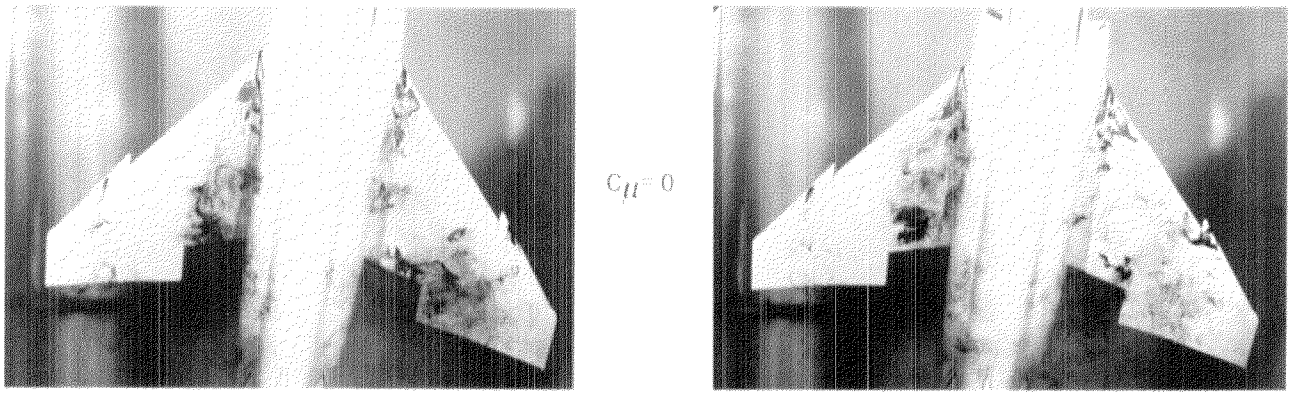

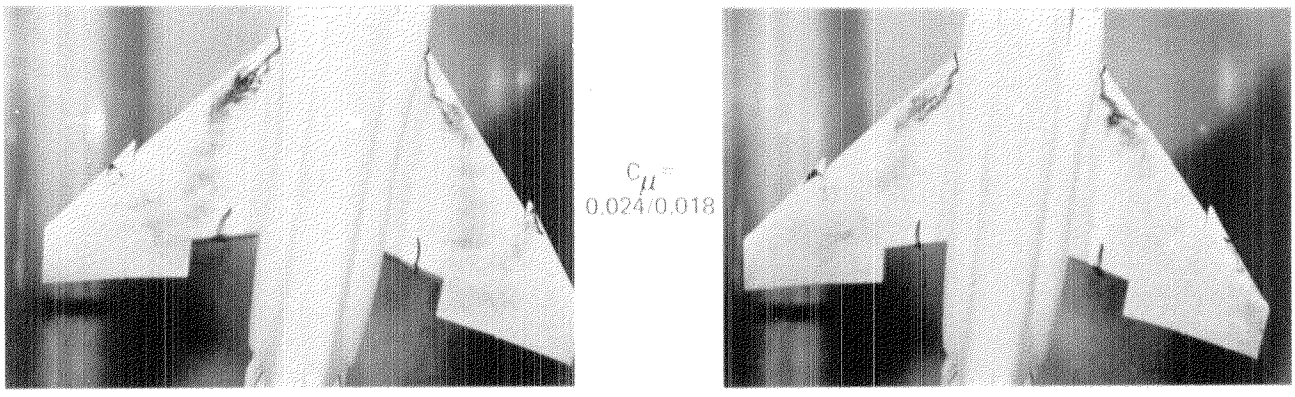

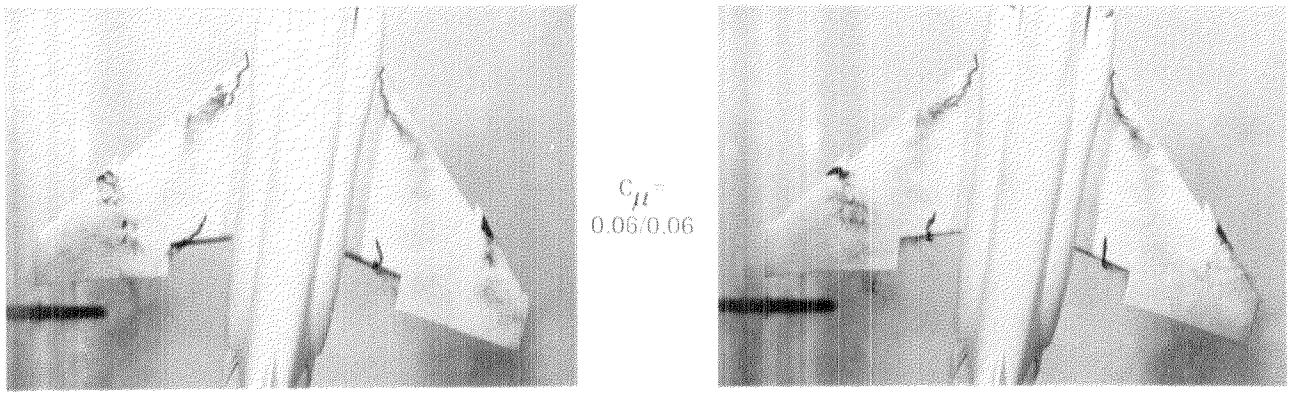

$\alpha = 25^0$ $\alpha = 30^0$

FIGURE 16. CONCLUDED

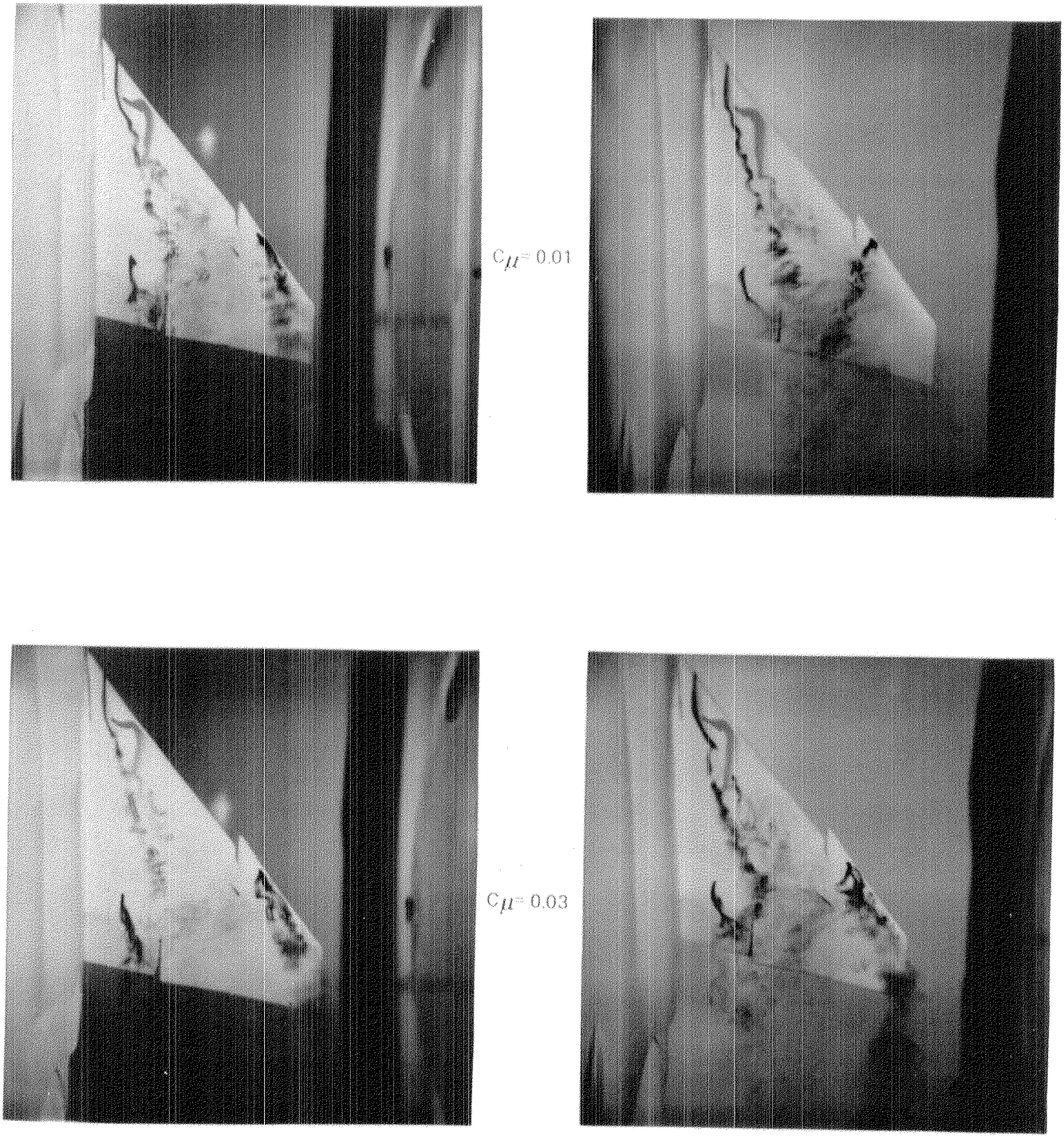

FIGURE 17. EFFECT OF SWEEP ANGLE AND CHORDWISE LOCATION OF THE OUTBOARD NOZZLE FOR $\alpha = 18^o, \delta_n/\delta_f = 15^o/15^o$

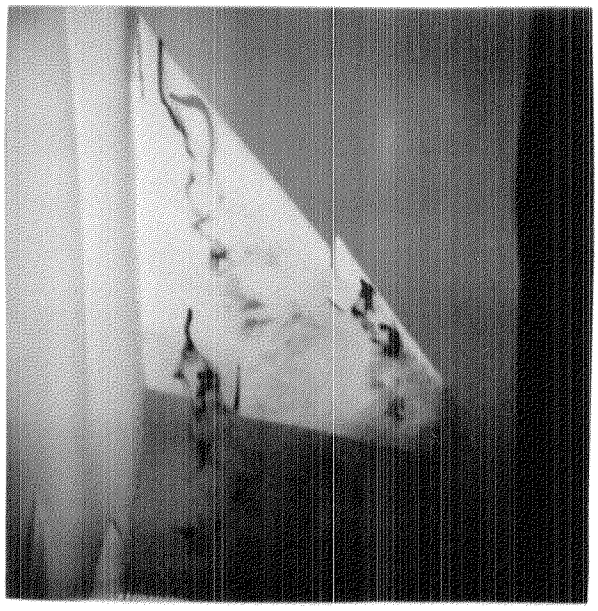

$C_\mu = 0.01$

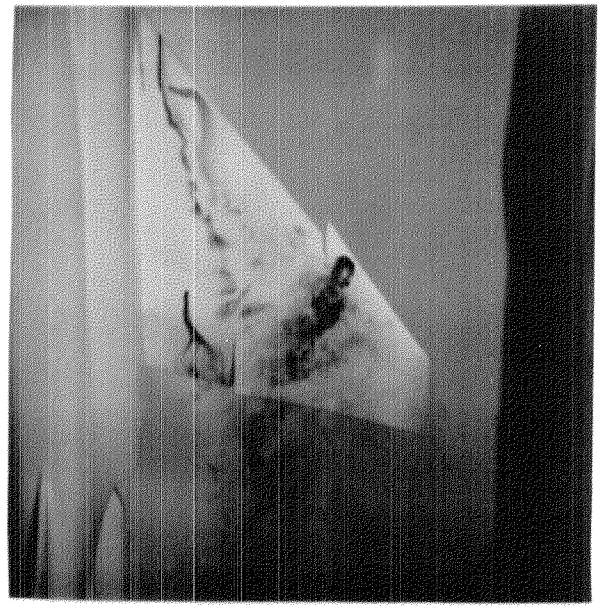

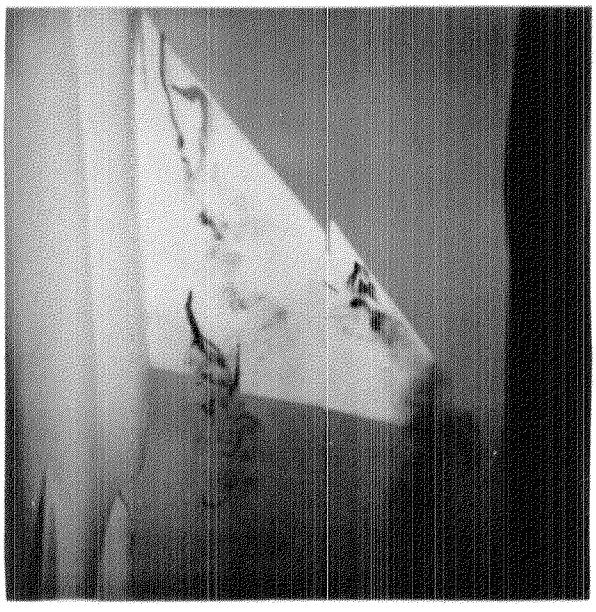

$C_\mu = 0.03$

$\Lambda_N = 43.6^o$, $x/c_h = 0.25$

$\Lambda_N = 43.6^o$, $x/c_h = 0.35$

FIGURE 17. CONCLUDED

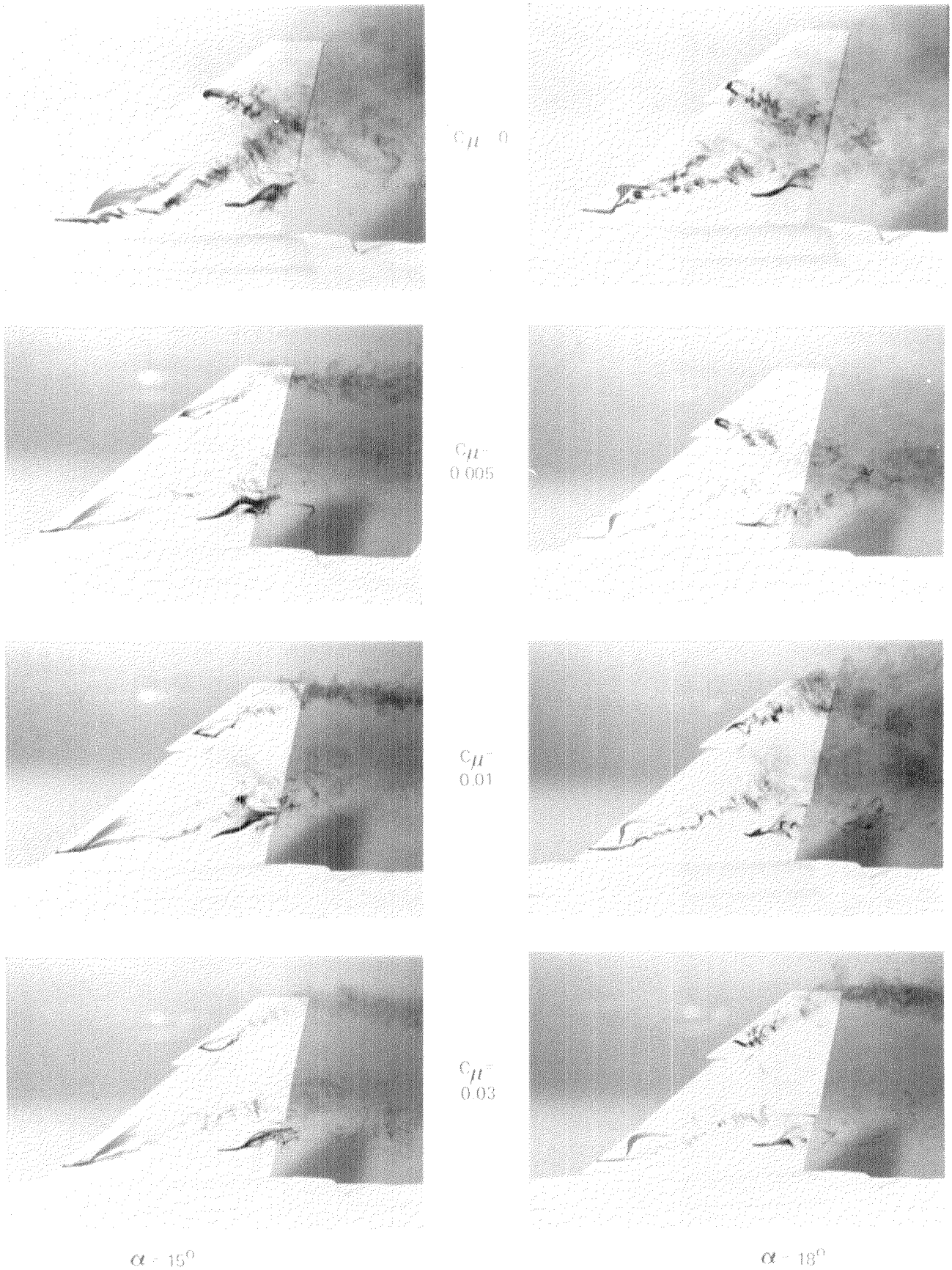

FIGURE 18. SPANWISE BLOWING OVER THE OUTBOARD WING PANEL FOR $x/c_h = 0.25, \Lambda_N = 53.6^o, \delta_n/\delta_f = 15^o/15^o$

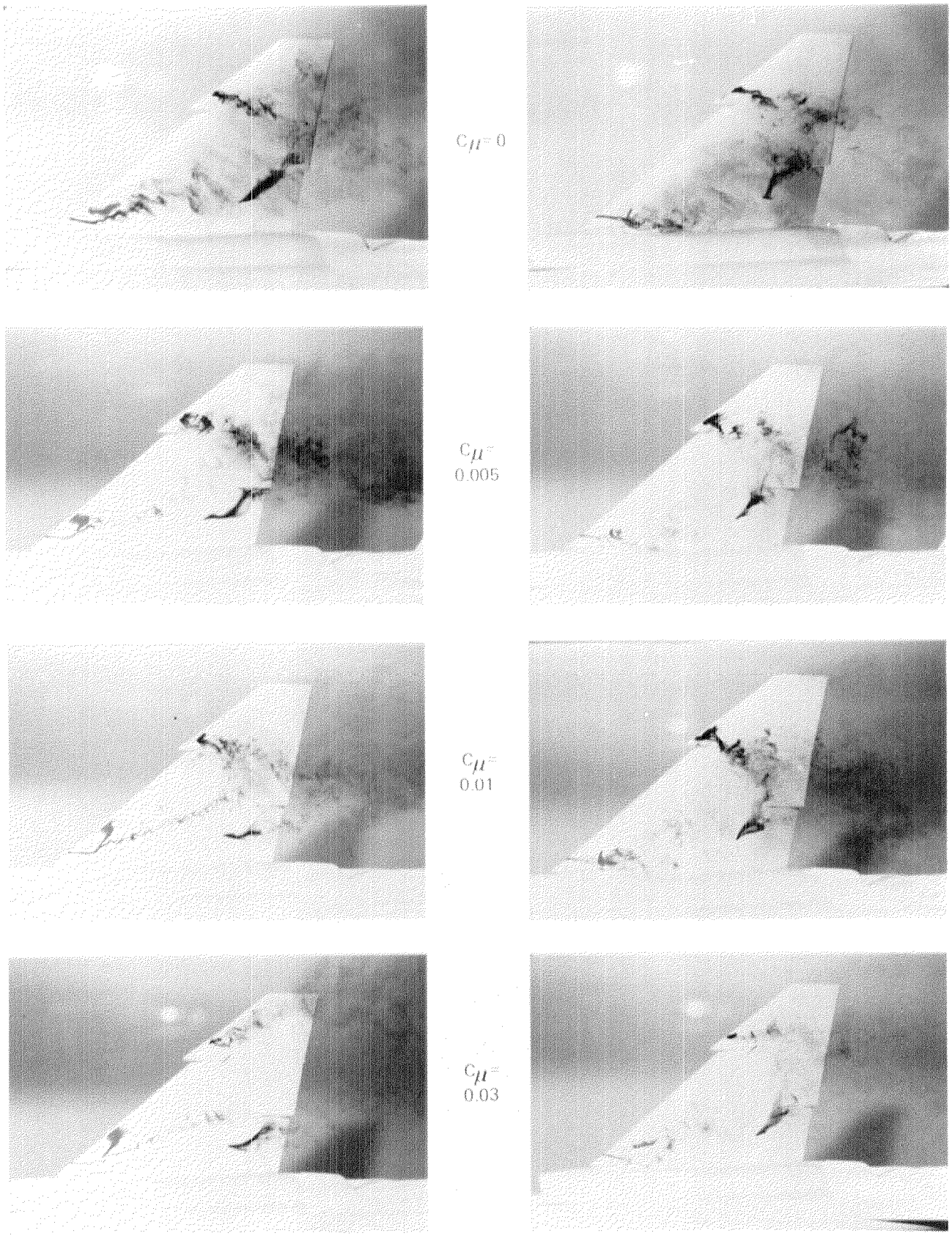

FIGURE 18. CONCLUDED

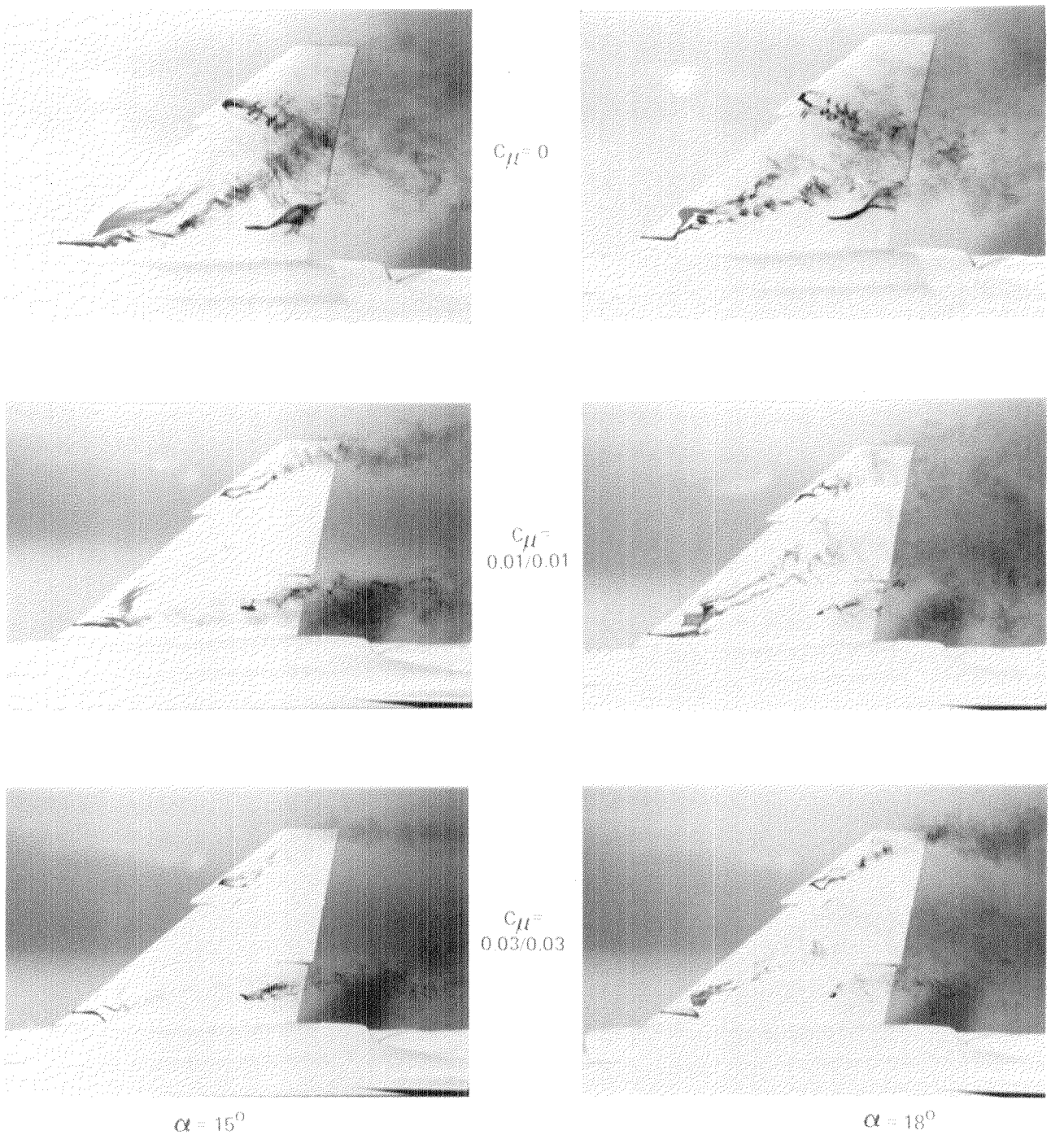

FIGURE 19. SPANWISE BLOWING OVER INBOARD AND OUTBOARD WING PANELS FOR $x/c_r = 0.13$, $x/c_h = 0.25$, $\delta_n/\delta_f = 15^o/15^o$

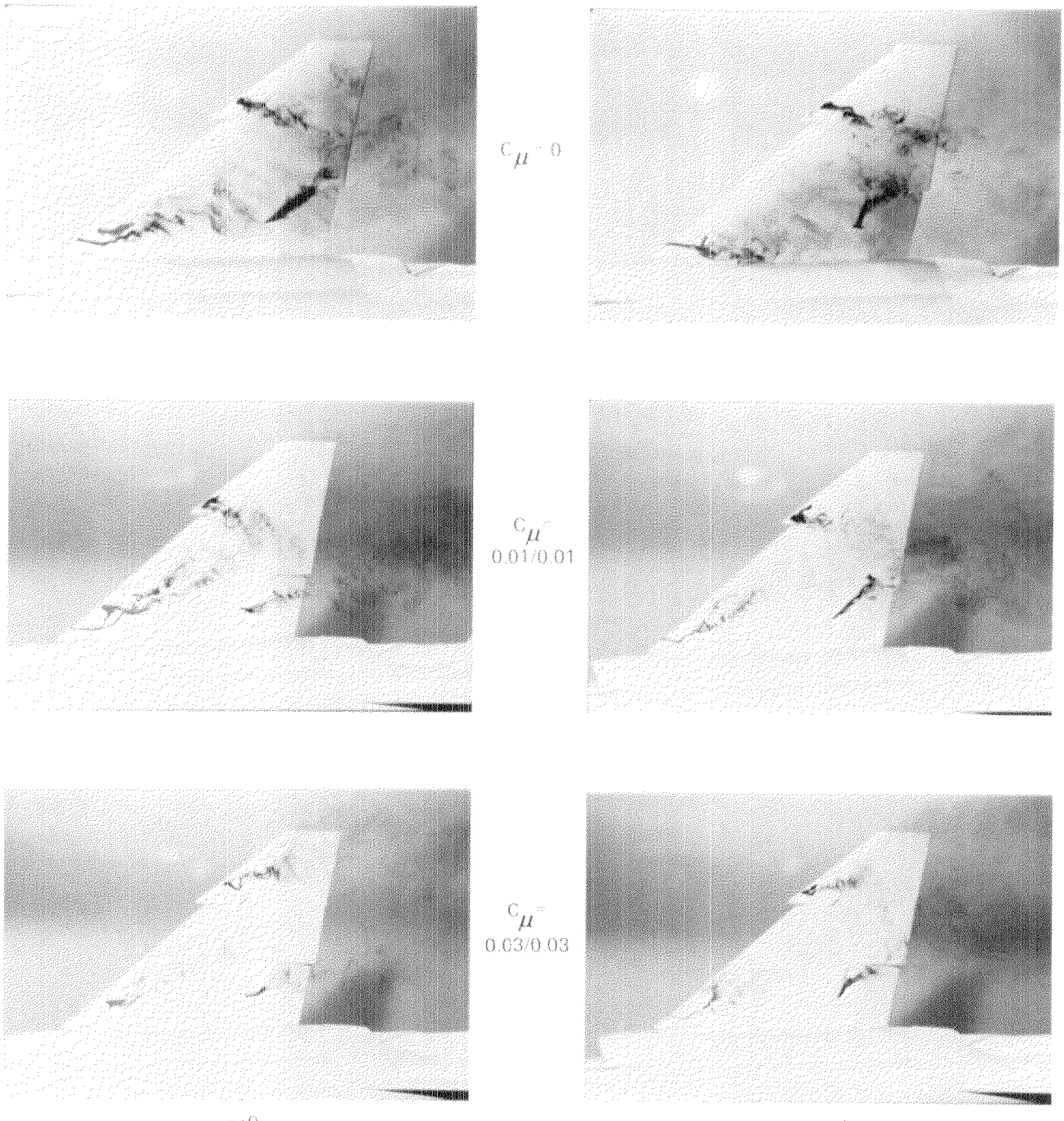

FIGURE 19. CONCLUDED

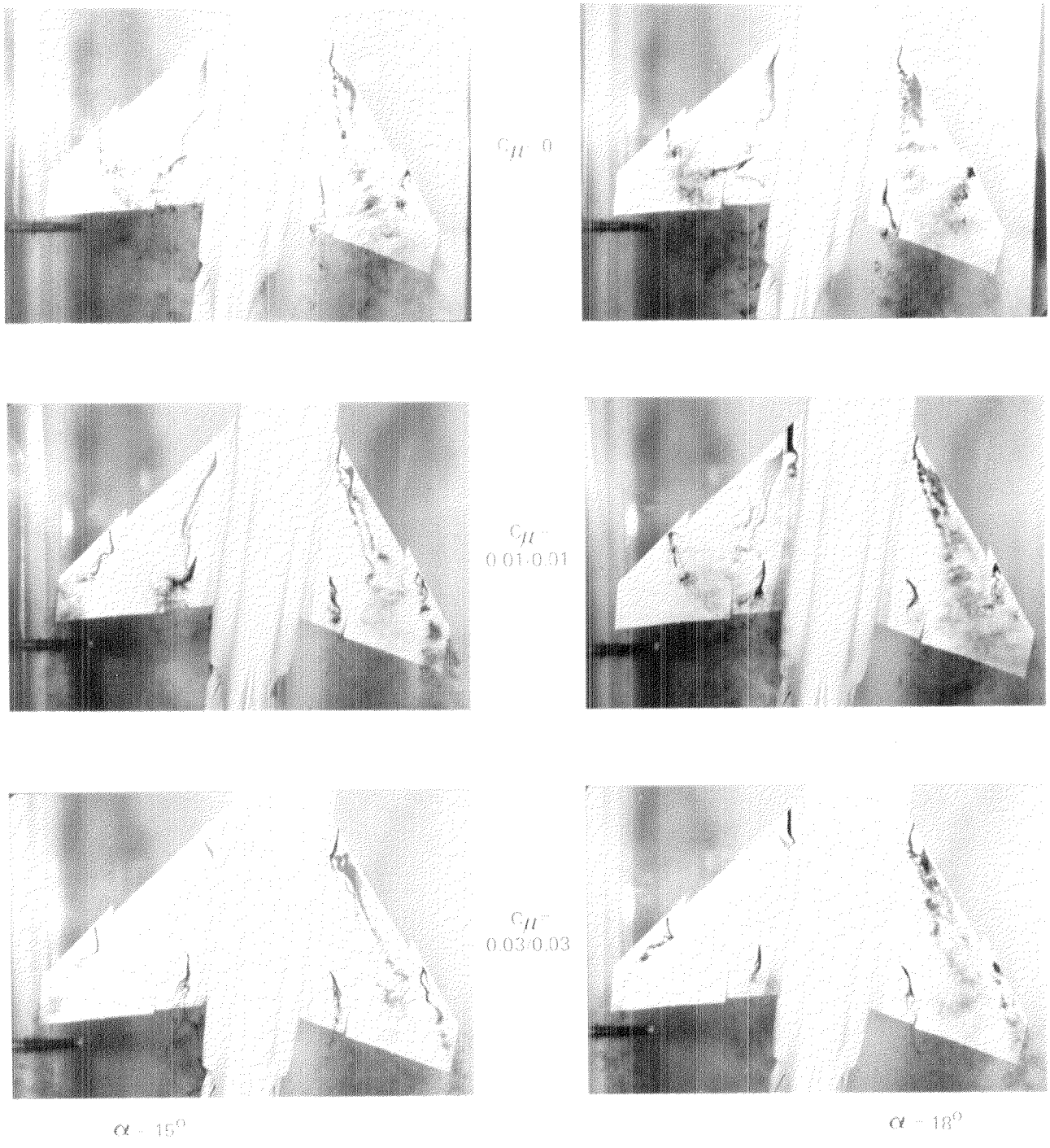

FIGURE 20. SPANWISE BLOWING OVER INBOARD AND OUTBOARD WING PANELS IN SIDESLIP WITH $x/c_r = 0.13$, $x/c_h = 0.25$, $\delta_n/\delta_f = 15^o/15^o$, $\beta = -10^o$

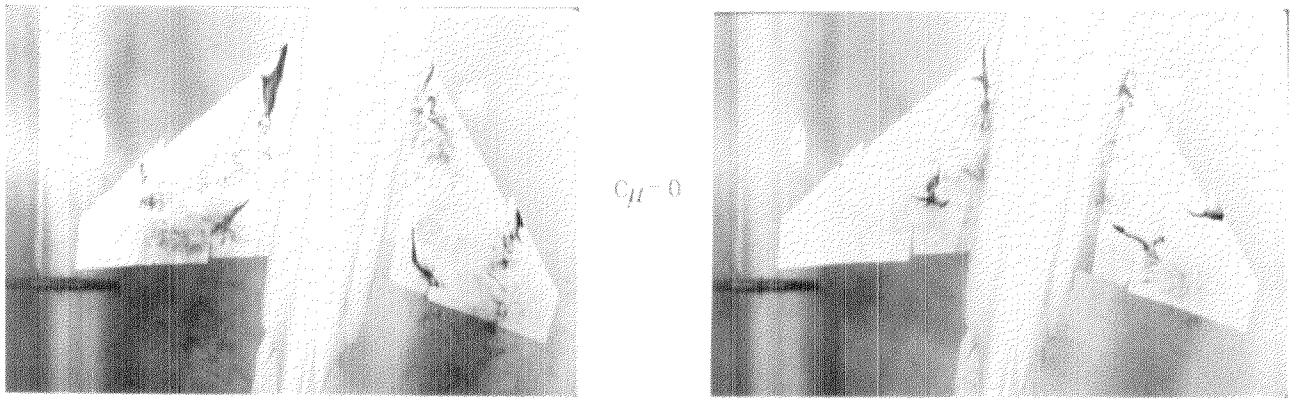

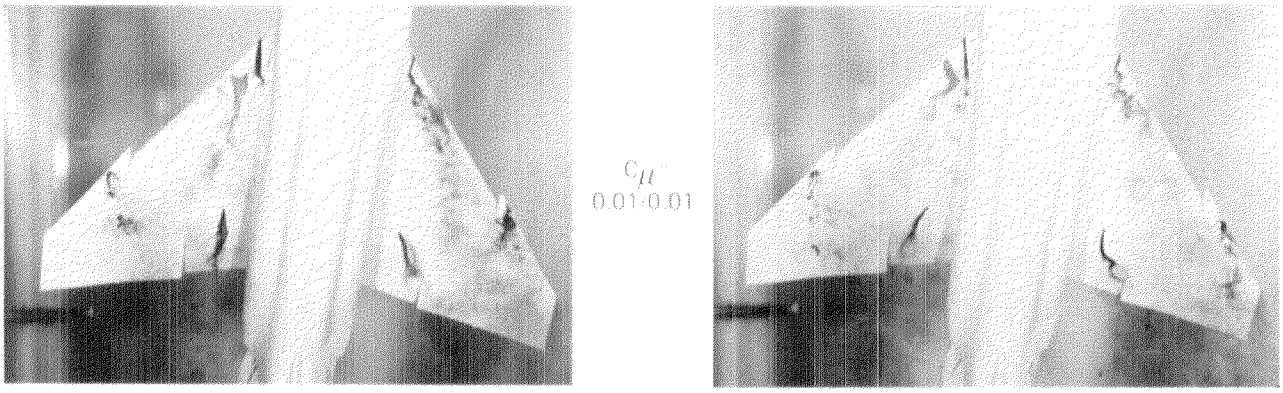

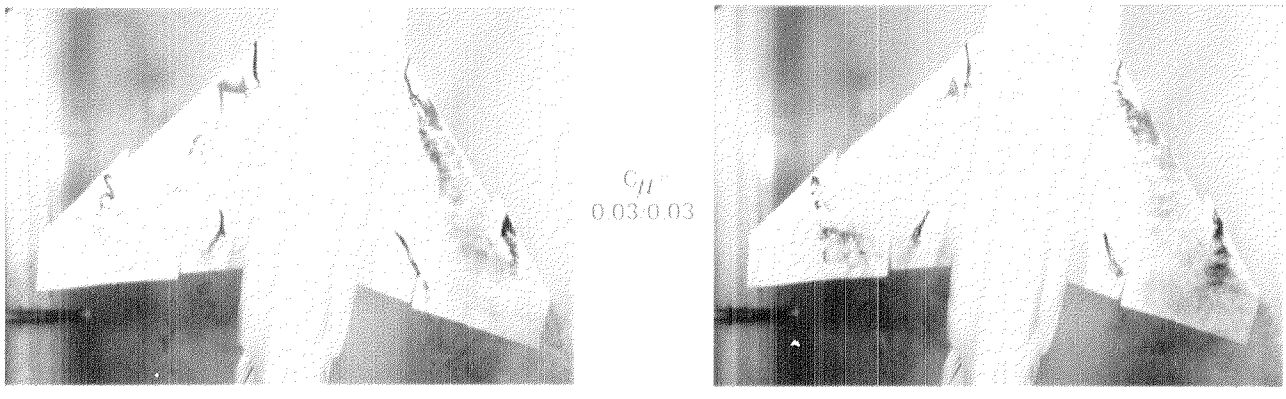

$\alpha = 20^\circ$ $\alpha = 25^\circ$

FIGURE 20. CONCLUDED

1 Report No	2 Government Accession No	3 Recipient's Catalog No
NASA CR-163096		

4 Title and Subtitle	5 Report Date
FLOW VISUALIZATION STUDY OF SPANWISE BLOWING APPLIED TO THE F-4 FIGHTER AIRCRAFT CONFIGURATION	August 1980
	6 Performing Organization Code

7 Author(s)	8 Performing Organization Report No
Dale J. Lorincz	NOR 80-138
	10 Work Unit No
	505-31-44

9 Performing Organization Name and Address	11 Contract or Grant No
Northrop Corporation Aircraft Division 3901 West Broadway Hawthorne, California 90250	NAS4-2616
	13 Type of Report and Period Covered
	Contractor Report-Topical

12 Sponsoring Agency Name and Address	14 Sponsoring Agency Code
National Aeronautics and Space Administration Washington, D.C. 20546	H-1127

15 Supplementary Notes

NASA Technical Monitor Edward L. Friend, Dryden Flight Research Center

16 Abstract

Water tunnel studies have been performed to qualitatively evaluate the benefits of spanwise blowing applied to the F-4 fighter aircraft. Particular emphasis was placed on defining the changes that occurred in the vortex flow fields above the wing due to spanwise blowing over the inboard and outboard wing panels and over the trailing-edge flaps. The flow visualization tests were conducted in the Northrop water tunnel using a 1/48-scale model of the F-4. Flow visualization photographs were obtained for angles of attack up to 30° and sideslip angles up to 10°.

Spanwise blowing on the F-4 model was investigated in detail to determine the sensitivity of the vortex flows to changes in flap deflection angle, nozzle position, and jet momentum coefficient. Deflection of the leading-edge flap delayed flow separation and the formation of the wing vortex to higher angles of attack. Spanwise blowing was found to delay the breakdown of the wing vortex to farther outboard and to higher angles of attack. Spanwise blowing over the trailing-edge flap entrained flow downward, which produces a lift increase over a wide range of angles of attack.

The sweep angle of the windward wing was effectively reduced in sideslip. This decreased the stability of the wing vortex, and it burst farther inboard. Reduced wing sweep required a higher blowing rate to maintain a stable vortex. A vortex could be stabilized on the outboard wing panel when an outboard blowing nozzle was used. Blowing from both an inboard and an outboard nozzle was found to have a favorable interaction.

17 Key Words (Suggested by Author(s))	18 Distribution Statement
Spanwise blowing Leading-edge vortex enhancement High angle of attack aerodynamics Vortex flow fields	Unclassified - Unlimited Subject category: 02

19 Security Classif (of this report)	20 Security Classif (of this page)	21 No of Pages	22 Price*
Unclassified	Unclassified	88	

* For sale by the National Technical Information Service, Springfield, Virginia 22161

End of Document